

Invited Paper

Plastic Optical Fibers: An Introduction to Their Technological Processes and Applications

Joseba Zubia and Jon Arrue

ETSI de Bilbao (School of Telecommunications Engineering), Departamento de Electrónica y Telecomunicaciones. Alameda de Urquijo s / n 48013-Bilbao, Spain

E-mail: jtpzuzaj@bi.ehu.es

Received December 6, 2000

The most significant features of plastic optical fibers (POFs) are reviewed, including the main types of POFs, their manufacture, and their possible present and future applications. Among others, their properties regarding bandwidth, attenuation, and influence of external parameters are discussed. These fibers serve as a complement for glass fibers in short-haul communications links, because they are easy to handle, flexible, and economical. Because of these merits, varied applications with POFs have been developed and commercialized, from their use as a simple light transmission guide to their utilization as sensors and telecommunications cables. This paper is a comprehensive introduction to POFs. In addition, its great number of references facilitates further inquiries about the subject. © 2001 Academic Press

1. INTRODUCTION

During the past 30 years a new type of optical fiber has been researched, namely the *plastic optical fiber (POF)*. The situation of this transmission medium had remained rather stagnated for years because of its high attenuation and the lack of demand of specific commercial applications. However, since the development of the graded-index plastic optical fibers by Professor Koike at Keio University (1990) and the later attainment of the low-attenuation perfluorinated fibers (1996), plastic optical fibers have received a lot of interest, which is expected to give rise to a great deal of applications in the next several years. This paper serves as a concise

introduction to the most significant features of POFs, their historical evolution, and their propagation properties.

2. PLASTIC OPTICAL FIBERS (POFs)

2.1. Historical Evolution

Since the invention of the telegraph by Samuel Morse in 1838 an increasingly larger portion of the electromagnetic spectrum has been utilized for conveying information from one place to another. The reason for this is that, in electrical systems, data are usually transferred through the communications channel by superimposing the information signal onto a sinusoidally varying electromagnetic wave, which is known as the carrier. Since an increase in the carrier frequency provides a larger information capacity [1], the historical trend in telecommunications systems has been to employ progressively higher frequencies. At the destination, the information is removed from the carrier wave and processed as desired. Because of its high frequencies, the optical portion of the electromagnetic spectrum is currently being used for most of the communications links by employing optical fibers as transmission media. Specifically, the well-known plastic optical fibers with PMMA core were introduced in the 1960s, although the first optical fibers that were used as a communications channel were made of glass. In the past several decades, concurrent with the successive improvements in glass fibers, POFs have become increasingly popular, owing to their growing utility [2].

Although POFs have been available for some time, only quite recently have they found application as a high-capacity transmission medium, thanks to the successive improvements in their transparency and bandwidth [3]. At present, they are advantageously replacing copper cables in short-haul communications links by offering the advantages intrinsic to any optical fiber in relation to transmission capacity, immunity to interference and small weight. In addition, POFs serve as a complement for glass fibers in short-haul communications links because they are easy to handle, flexible, and economical, although they are not used for very long distances because of their relatively high attenuation. These characteristics make them especially suitable as a means of connection between a large net of glass optical fiber and a residential area, where distances to cover are generally less than 1 km. An example would be Internet access from home or from an office. For this purpose, POFs allowing for increasingly better features regarding distance and transmission speed have been manufactured. Nowadays, with the PMMA-core optical fibers, transmissions at 156 Mb/s over distances up to 100 m can be carried out [4], and transmission speeds of 500 Mb/s over 50 m can be reached [5]. To achieve higher transmission speeds graded index POFs can be used [6]. In addition, a special type of POF made from an amorphous fluorinated polymer called CYTOP and developed by Koike and Asahi Glass will be soon available in the market [7]. This new fiber presents a considerably lower attenuation than the common POFs (≈ 30 dB/km), which allows the transmission distance to be increased up to 1 km for a transmission speed of 1.2 Gb/s/km. Figure 1 shows the historical evolution of the first POFs, including the core material and the optical

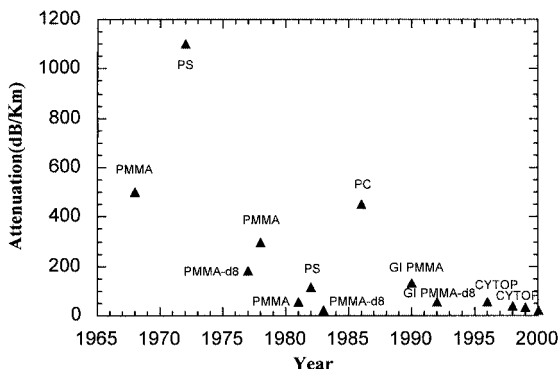


FIG. 1. Historical evolution of the attenuation of POFs during the past 30 years as a function of the core constituent material.

power attenuation per kilometer of fiber at a wavelength of minimum attenuation (i.e., at a transmission window). Table 1 shows the most significant landmarks of POFs during the past 30 years.

As we have already mentioned, POFs present some important advantages over their glass counterparts. Specifically, their large diameter (typically 0.25–1 mm) allows low precision plastic connectors to be used, which reduces the total cost of the system. In addition, POFs stand out for their greater flexibility and resistance to impacts and vibrations, as well as for the greater coupling of light from the light source to the fiber. Because of these merits, varied applications with POFs have been developed and commercialized, from their use as a simple light transmission guide in displays to their utilization as sensors and telecommunications cables.

In the field of sensors, numerous types of products based on POFs have been commercialized [8], for example, scanning heads, shape-defect detectors used in bottling plants, and liquid-level detectors. In addition, by using conventional POFs, it is possible to make sensors measure distance, position, shape, color, brightness, opacity, density, turbidity, etc. [9, 10]. These sensors can serve to control the various manufacturing parameters in automated production processes with robots. On the other hand, the development of fluorescent POFs has enabled sophisticated sensors such as those utilized for particle tracking to be made [11]. In the field of data transmission, POFs are especially suitable for short-haul communications links requiring a large number of connections, as usually happens in cars and trains, inside the buildings of some companies or in local area networks. Because of their large diameter, POFs are easier to install and align than their glass counterparts [2, 12].

2.2. POF Structure

POFs used for optical communications are highly flexible waveguides composed of nearly transparent dielectric materials. The cross-section of these fibers is circular and, generally, divisible into three layers, as shown in Fig. 2. The three layers are called the *core*, *cladding*, and *jacket*, a protective cover. Within the core,

TABLE 1
Historical Evolution of the Most Important Landmarks Related to POF
during the Past 30 Years

Year	Organization	Landmark
1968	Dupont	First SI POF with PMMA core
1972	Toray	First SI POF with PS core
1981	NTT	Low attenuation PMMA SI POF (55 dB/km at 568 nm)
1982	Keio University	First GI POF (1070 dB/km at 670 nm)
	NTT	First SI POF with deuterated PMMA core (20 dB/km at 650 nm)
1983	Mitsubishi Rayon	PMMA "Eska" SI POF (110 dB/km at 570 nm)
1987	France	The French POF Club is established
1990	Keio University	First high speed transmission with a PMMA-core GI POF (300 MHz*km at 670 nm)
1991	Hoechst Celanese	SI PMMA "Infolite" POF (130 dB/km at 650 nm)
1992	Keio University	GI deuterated PMMA POF (55 dB at 688 nm)
1993	Essex University	Transmission at 631 Mb/s over 100 m by means of a PMMA-core SI POF and an equalizer circuit
1994	USA/Japan	The high speed POF Network (HSPN) Consortium is created
	Keio University,	The POF Consortium of Japan is created
	IBM	Transmission at 1 Gb/s over 30 m by means of a GI POF and a VCSEL at 670 nm
	Keio University,	Transmission at 2.5 Gb/s over 100 m by means of a GI POF at 650 nm; First multicore SI POF for high speed transmission
	NEC	
	Asahi Chemical	
1995	Mitsubishi Rayon,	Transmission at 156 Mb/s over 100 m by means of a low NA SI POF and a fast red LED
	NEC	
1996	Keio University,	First perfluorinated (PF) GI POF (50 dB/km at 1300 nm)
	KAST	Theoretical estimation of the losses in a PF POF (0.3 dB/km at 1300 nm)
		Theoretical estimation of the transmission speed in a GI POF optical link (PMMA: 4 Gb/s over 100 m; PF: 10 Gb/s over 1 km)
1997	POF Consortium of Japan	Standardization at ATM LAN (156 Mb/s over 50 m of SI POF) in the ATM Forum.
		Standardization of the norm IEEE 1394 (156 Mb/s over 50 m of SI POF)
	Keio University,	Transmission at 2.5 Gb/s over 200 m by means of a PF-core GI POF at 1300 nm
	Fujitsu, Asahi Glass	
1998	COBRA, Eindhoven University, Keio University, Asahi Glass, NEC	Transmission at 2.5 Gb/s over 300 m by means of a PF-core GI POF at 645 nm
	Matsushita	Transmission at 500 Mb/s over 50 m by means of a GI POF and a fast red-color LED (RC-LED; 650 nm)
1999	COBRA, Eindhoven University, Keio University, Asahi Glass	Transmission at 2.5 Gb/over 500 m by means of a PF-core GI POF at 840 and 1310 nm
	University of Ulm,	Transmission at 7 Gb/s over 80 m by means of a PF-core GI POF at 950 nm
	Asahi Glass	
	Bell Laboratories,	11 Gb/s data transmission through 100 m of perfluorinated GI POF at 830 nm and 1310 nm.
	Asahi Glass	
2000	Asahi Glass	GIPOF (Lucina) with an attenuation of 16 dB at 1300 nm and 569 MHz*km

Note: SI, step-index; GI, graded-index; PMMA, polymethyl methacrylate; PS, polystyrene; PF, perfluorinated fiber.

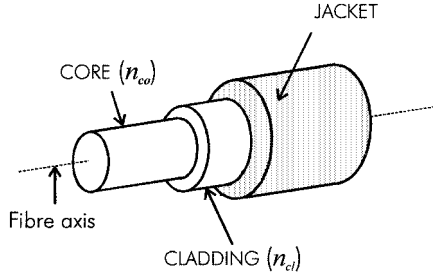


FIG. 2. Structure of a POF.

the refractive-index profile can be uniform (step-index fibers, SI) or graded (graded-index fibers, GI), while the cladding index is typically uniform (Fig. 3).

The core radius a usually ranges between 125 and 490 μm [12]. Most of the light propagates along the core, which is achieved by surrounding the core with a cladding of a lower refractive index. Typical values for the core and cladding refractive indices in a step-index PMMA POF are, respectively, $n_{co} \cong 1.492$ and $n_{cl} \cong 1.417$ [2, 13]. In a graded-index POF the core refractive index varies with the distance r to the symmetry axis (Fig. 3), following the expression

$$\begin{aligned} n(r) &= n(0) \cdot \sqrt{1 - 2\Delta(r/a)^g} = n_{co} \cdot \sqrt{1 - 2\Delta(r/a)^g} & r \leq a \\ n(r) &= n(0) \cdot \sqrt{1 - 2\Delta} = n_{co} \cdot \sqrt{1 - 2\Delta} = n_{cl} & r > a, \end{aligned} \quad (1)$$

where the value of Δ is the *relative difference between indices*:

$$\Delta = \frac{n_{co}^2 - n_{cl}^2}{2n_{co}^2}. \quad (2)$$

The factor g is the so-called *profile exponent* of the optical fiber, because different index profiles are obtained by changing this exponent. For example, a parabolic profile is obtained for a value $g = 2$ and a step-index profile for the limit $g \rightarrow \infty$.

The jacket or coating carries out a function of mechanical protection for the optical fiber, providing robustness; it is generally made of polyethylene, although polyvinylchloride and chlorinated polyethylene can also be used. Table 2 summarizes the main parameters of the most frequently used POFs. Hard core silica (HCS) plastic clad fibers (PCS) are included for comparison.

2.3. Single-mode and Multimode Fibers

Optical fibers can be classified in two groups from the point of view of propagation: *single-mode fibers*, with a comparatively small core which requires the wave model of light, and *multimode fibers*, whose core is large enough to be analyzed with a geometric ray-tracing model. The frontier between the two groups is determined by means of the structural parameter V , which is given by

$$V = \frac{2\pi\rho}{\lambda} (n_{co}^2 - n_{cl}^2)^{1/2}, \quad (3)$$

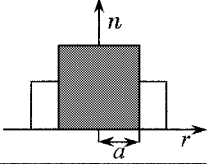
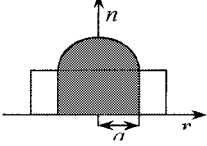
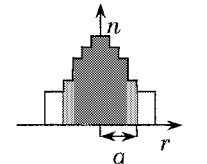
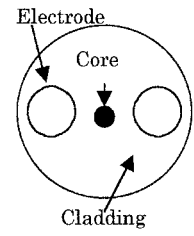
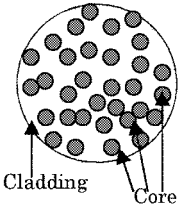
Index profile	Fiber type	Bandwidth*distance	Main features
	Single mode Multimode	3 MHz*Km	Step index profile; suitable for short haul communications High intermodal disper- sion
	Multimode	600 MHz*Km	Graded index profile; suitable for short and medium haul communi- cations Low intermodal disper- sion
	Multimode	30 MHz*Km	Multistep index profile; suitable for short and medium haul communi- cations. Low intermodal dispersion. Well suited for mass production.
Transverse section	Fiber type	Bandwidth*distance	Main features
	Single mode Electrooptic	---	Single mode POF with embedded electrodes Specially indicated for the design of modulators
	Multimode	55 MHz*Km	Multicore SI POF. Tremendous stability against bending ; POFs winded round a stick of 3 mm radius shows 0.0 dB when NA=0.25 and the core diameter is 130 μm.

FIG. 3. Types of refractive index profiles in POFs and their main features.

where λ is the wavelength of the light that propagates through the fiber (typically 650 nm with PMMA POFs and 850 and 1310 with perfluorinated (PF) POFs). When the value of the parameter V , called the *normalized frequency*, is higher than 2.405, it can be proved that the behavior of step-index fibers is multimode [14, 15]; for large values of V , the number of propagation modes in a step-index fiber is given, according to the electromagnetic theory, by the following expression:

$$N = \frac{V^2}{2} \quad \text{if } V \gg 1. \quad (4)$$

TABLE 2
Comparison of Several Parameters Corresponding to POFs of
Different Core Composition

Material	Attenuation (dB/km)	Bandwidth (GHz*km)	Application	Core/cladding refractive indices	NA	Core diameter (μm)
PMMA	55 (538 nm)	0.003	LANs, industrial communications and sensing	1.492/1.417	0.47	250–1000
PS	330 (570 nm)	0.0015	High T industrial short haul communications and sensing	1.592/1.416	0.73	500–0000
PC	600 (670 nm)	0.0015	High T communications and sensing	1.582/1.305	0.78	500–1000
CYTOP	16 (1310 nm)	0.59 (GIPOF)	LANs	1.353/1.34		125–500
PCS HCS	5–6 (820 nm)	0.005	Communications, medical, industrial and sensing	1.46/1.41	0.40	110–1000

Note: PMMA, polymethyl methacrylate; PS, polystyrene; PC, polycarbonate; CYTOP is an amorphous flourinated polymer; HCS, hard core silica; PCVS, plastic clad silica.

Each mode represents a solution to Maxwell's equations. For a typical POF link, it can be obtained that the approximate number of modes is $N \approx 10^4$ – 10^6 . This high value of N enables us to analyze POFs by means of a geometric model, replacing the concept of mode used in the electromagnetic theory of light by the concept of light ray. The results obtained with this model become more exact as the number of rays considered increases, provided that the theoretical number of modes N , calculated as above, is not exceeded [15]. An important consequence of this huge number of rays is that light polarization is not preserved along the fiber. There is no correlation between input and output polarization states, except for very short POFs (< 0.5 m) [16, 17].

Single-mode POFs (SMPOFs) have also been developed by Koike *et al.* [18]. However, they exhibit a much larger attenuation than single-mode glass fibers and they lack the main advantage of conventional POFs, i.e., easiness to handle and low cost connectors. For all these reasons, research in this field is not very active. However, there is some work that is worth mentioning. For example, Sentel Technologies sells SMPOFs for 1300 nm with a PMMA cladding and a copolymer PS/PMMA core [19]. Typical core sizes for single-mode operation range from 5 to 20 μm with an outer cladding diameter between 100 and 800 μm . These fibers can be easily coupled to planar waveguides and they serve as components for some devices such as sensors. The core can be doped with a dye to control absorption or nonlinear propagation properties.

A variety of the SMPOF is the electro-optic SMPOF (ESMPOF). These are doped fibers that are drawn while polarizing the core using indium electrodes. As a consequence, the center of inversion symmetry of the molecules (dyes) is broken,

which results in a second order susceptibility. The structure of ESMPOF is shown in Fig. 3. Although the alignment of the dyes in the core decays with time, which results in a decay of the electro-optic response, the core can be repolarized [19, 20].

The other variety is the dual core dye-doped single mode POF, or, in brief, DCSMPOF. It consists of two dye-doped PMMA cores, surrounded by a circular cladding of PMMA. The dye is squarylium (ISO). When the cores are closely positioned, the DCSMPOF behaves as a coupler or a spectral filter. If they are separated, they serve to detect strain, displacement, and temperature because of the changes induced in the relative light path. Typical coupling lengths are close to 9 mm. Most of DCSMPOFs are step index, but graded index profiles can be manufactured as well, by controlling dye diffusion. DCSMPOFs can also be used to design ultrafast all-optical switches and nonlinear couplers [20, 21].

2.4. Manufacturing Techniques of POFs

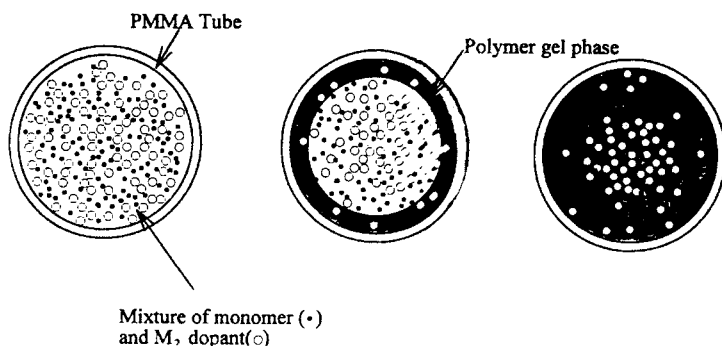
Two steps are followed in the manufacture of POFs. First, a solid cylindrical rod, called *preform*, is made, which is approximately .5–1 m long and several centimeters in diameter; the structure of this preform will determine the core and cladding refractive index profiles. The second step consists in extruding the preform, which yields a POF length in the range between half a kilometer and several kilometers [2]. Production techniques have advanced as much as to enable the manufacture of inexpensive high-quality low-loss POFs [12, 22–25].

Step-index POFs are manufactured by means of a melt spinning process in which fibers are obtained by either continuous or batch extrusion. In the continuous extrusion process, a monomer, an initiator, and a chain transfer agent are continuously fed into the reactor and the fiber is continuously withdrawn from the die. This is an efficient process since high production rates are possible.

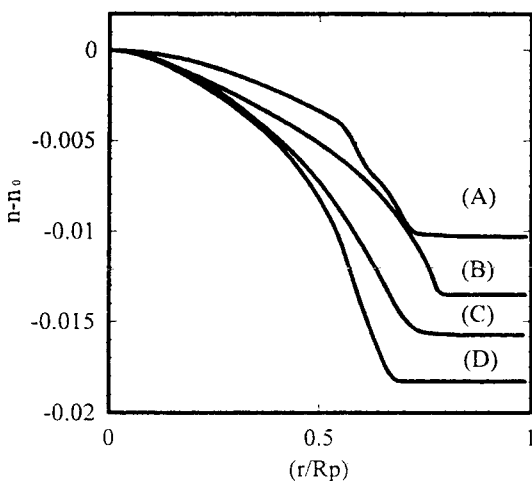
To obtain any other particular refractive index profile in the core along the radial direction, a preform with the desired profile can be employed. In practice, when more complex refractive index profiles are required, such as graded-index ones, a technique based on drawing a preform by melting its tip with the aid of an oven is used. The preform is a cylinder of polymer whose refractive-index distribution can be made to coincide with that desired for the POF's core, so this technique is very versatile.

At present there are two main techniques to produce GI POFs: the interfacial gel polymerization technique [6] and the diffusion technique [26]. The former process requires the manufacture of a hollow cylinder made of polymer, e.g., PMMA, which will be the POF's cladding. Next, the hollow cylinder is filled with a mixture of the monomer from which the polymer cylinder was made, a dopant with higher refractive index than that of the polymer, an initiator, and a chain transfer agent. The filled cylinder is then heated to 95°C and rotated on its axis for 24 h. During this time the inner wall of the cylinder widens slightly, as a consequence of the formation of a gel phase on it. Due to the so-called *gel effect*, the polymerization reaction is accelerated in this zone; i.e., the polymer is gradually formed from the gel phase on the inner wall of the tube. The reaction is completed when the initially hollow cylinder becomes a solid cylinder. The reason it is necessary to use

dopants with higher refractive index than that of the polymer is that light should be confined in the structure. Koike *et al.* [6, 26] have used several dopants, both for the tube and for the inner mixture (Fig. 4a). Table 3 lists some of the materials used by these researches to produce GI POFs. The mechanism for the correct distribution of the refractive index consists in the selective diffusion of monomer and dopant material in the gel-polymer phases created in the inner wall of the tube. The molecular volume of dopants is higher than that of the monomer, which enables the monomer to diffuse faster than the dopant inside the gel phase. For this reason, dopant molecules are concentrated in the central region of the cylinder, so the refractive index is higher in this region. Depending on the dopants, their movement will be different from each other, which will result in different distributions of the index of refraction. Fig. 4b shows the distributions obtained with four different dopants.



(a)



(b)

FIG. 4. (a) Schematic representation of the selective diffusion of monomer and M_2 dopant molecules into polymer gel phase to form the graded index distribution. (b) Refractive index distribution of the MMA-M₂ dopant system GI preform. (a) MMA-BB system. (a) MMA-BEN system. (a) MMA-BBP system. (a) MMA-DPP system (after Koike *et al.* [6]).

TABLE 3
Dopants Used to Make Graded Index POFs

	Material	Index of refraction*	Density g/cm ³	Molecular volume Å ³	Molecular weight g/mol	Volume Å ³
Tube	PMMA	1.492	—	—	—	—
Dopant	BB	1.60	1.49	173.8	157	109
	BBP	1.540	1.10	471.7	312.4	305.2
	DPS	1.633	1.12	276.3	186.3	—
	DPP	—	—	336.4	318.3	294.4
	TPP	1.536	—	449.2	326.3	—
	BEN	1.568	—	314.6	212.3	208.7
	MMA	1.492	0.94	176.4	100.1	105.0

Note: BB, bromobenzen; BBP, benzyl *n*-buytl phthalate; DPS, diphenyl sulfure; BEN, benzyl benzoate; DPP, dyphenil phthalate; TPP, triphenyl phosphate; MMA, methyl methacrylate. The value of the refractive index corresponds to the yellow line of sodium.

2.4.1. Drawing of the POF

Once the preform has been obtained, it is held up by a support in the fiber extrusion tower (Fig. 5). The lower end of the preform is heated with the aid of a furnace to a temperature of approximately 200°C, so that it should acquire the necessary viscosity to be able to extrude it downward. The extrusion velocity and the speed at which the mandrel rotates are adjusted by a regulatory mechanism in order for the fiber to have the desired constant diameter.

During the extrusion process, the geometrical relationships between the core and the cladding are kept constant even though there may be a reduction of 300 to 1 from the diameter of the preform to the final diameter of the extruded fiber.

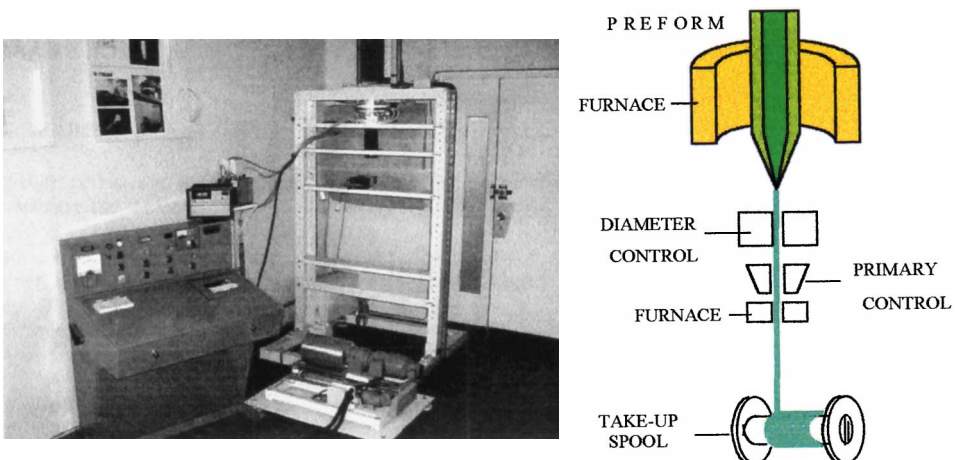


FIG. 5. Drawing out of the optical fiber (photo courtesy of LGE Toulouse).

Directly the fiber diameter is verified, and a coating is applied to the fiber. The plastic coating protects the optical fiber against microcurvatures, improves its mechanical resistance, and facilitates its handling. When the coating has hardened by the effect of heat or ultraviolet radiation, the optical fiber's resistance to traction is continuously tested by forcing the coated POF to pass through a series of pulleys that exert a mechanical tension on it, which is adjustable to a high degree of precision. In this way, the optical fiber must resist a minimum of load before being wound onto a cylindrical drum.

2.5. Attenuation

In a straight optical fiber, the power decreases exponentially with the distance z , as shown in the following expression:

$$P(z) = P(0)10^{-\alpha \cdot z/10}. \quad (5)$$

The value of α is called the *attenuation coefficient* of the optical fiber, and it expresses the value of the attenuation as a function of the fiber length. The expression for the attenuation in decibels is given by:

$$\alpha = -\frac{1}{z} 10 \cdot \log \frac{P(z)}{P(0)} \text{ dB/km}. \quad (6)$$

Figure 6 shows the spectral attenuation of two different materials used for the POF's core [2]. For the PMMA POF two absolute minima of attenuation can be

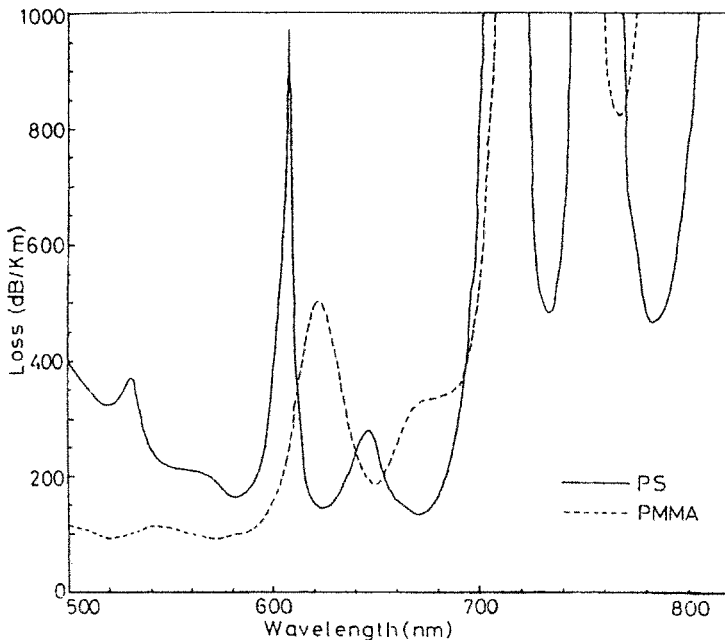


FIG. 6. Transmission loss spectra for PMMA and PS core POFs (from [2]).

observed, both of 70 dB/km, located at 522 and 570 nm (green), although there is a relative minimum around 650 nm (red).

The polystyrene (PS) POF ($n_{co} = 1.59$) has similar applications to those of the PMMA POF, but its minimum of attenuation is located in the red region. From a mechanical point of view, these fibers are better than those made of PMMA, although they have a higher attenuation. While their core is PS, their cladding is usually PMMA. Another fiber is the polycarbonate (PC) POF ($n_{co} = 1.5-1.59$), which is a high-temperature-resistant fiber. Its minimum of attenuation is found to be 600 dB/km and it is located at 770 nm. This kind of fiber can be used in industrial applications where the temperature is an important parameter.

The attenuation depends on the fiber core diameter, since it increases as the core diameter decreases. The attenuation at 570 nm is 70 dB/km for a 0.5 mm diameter PMMA POF and 130 dB/km for a 0.25 mm PMMA POF. This behavior is due to the greater number of geometrical and structural fiber imperfections for smaller diameters, among other causes. In practice, the manufacturing process is more difficult to control for smaller POF diameters (the thermal gradient is bigger), which results in a high number of imperfections. Besides, as the core diameter decreases, rays strike more frequently on the core-cladding interface (where imperfections are more frequent). Besides, due to the Göös-Hanchen effect, some of the power penetrates into the cladding, which has more attenuation, so power loss increases. Table 4 shows this effect for POFs made by several manufacturers.

Attenuation is also dependent on the spectral width and on the numerical aperture (NA) of the light source employed [9]. An increase in the spectral width or in the source's NA gives rise to higher attenuation [9, 27]. For instance, the attenuation of a PMMA POF is only 70 dB/km when the NA is 0.1, but 88 dB/km when the NA is 0.65.

The *transmission windows* are the regions of the spectrum where the POF's attenuation is minimum. They lie in the visible and near infrared range of the spectrum. Consequently, it is a common practice with PMMA POFs to use red lasers or fast high luminosity red LEDs, which lie in the window centered at 650

TABLE 4
Attenuation of PMMA SI POFs as a Function of the Core Diameter
and Different Manufactures

	Attenuation fiber diameter			
	250 μm (dB/km)	500 μm (dB/km)	750 μm (dB/km)	1000 μm (dB/km)
Mitsubishi	< 700	< 190	< 180	< 160
Toray	< 300	< 180	< 150	< 150
Asahi	—	< 180	< 180	< 125
Boston Optical Fiber	< 150	< 150	< 150	< 150
Optectron	< 150	< 150	< 150	< 150

nm. This is because LEDs or lasers having their emission spectra centered on relatively longer wavelengths are generally more powerful, which compensates for the higher POF attenuation at such wavelengths, provided that the transmission distance is not very large (for example, 100 m) [27].

The basic attenuation mechanisms in a POF can be classified into two main groups: *intrinsic* and *extrinsic*. Among the intrinsic losses, we have the *absorption* of the constituent material and the *Rayleigh scattering*. Both contributions depend on the composition of the optical fiber and, therefore, they cannot be eliminated. They represent the *ultimate transmission loss limit*. Basically, they are caused by the molecular vibrational absorption of the groups C—H, N—H, and O—H, by the absorption due to electronic transitions between different energy levels within molecular bonds and by the scattering arising from composition, orientation, and density fluctuations. Regarding the group of extrinsic losses, this is composed of those losses that would not appear in an ideal fiber. Among them, we find the absorption caused by both metallic and organic pollutants and the dispersion provoked by dust particles, microfractures, bubbles, and other structural imperfections in the POF [2]. Besides, there are also *radiation losses*, originated by perturbations (both microscopic and macroscopic) in the fiber geometry. Whenever the POF is bent with a finite curvature radius, radiation losses occur, although they are not significant unless this radius is small enough, e.g., only ten times as long as the fiber diameter. All of these mechanisms are classified in Table 5.

TABLE 5
Classification of the Loss Mechanisms That Contribute to the Fiber Attenuation

Type	Mechanism	Origin
Intrinsic	Absorption	Vibration modes
		Electronic transitions
	Rayleigh dispersion	Density fluctuations
		Orientation fluctuations
Composition fluctuations		
Extrinsic	Absorption	Transition metals
		Organic pollutants
	Dispersion	Dust
		Microfractures
		Bubbles
	Radiation	Structural imperfections
Microbends		
	Macrobends	

2.5.1. Intrinsic Losses

The vibrations of the molecular bonds C—H, N—H, and C=O constitute the most important source of intrinsic losses. This fact occurs because the fiber is made of polymer. The vibration frequencies of the bonds C—X, from a classic point of view, can be obtained from the expression

$$\lambda = 2\pi c \sqrt{\frac{\mu}{k}}, \quad (7)$$

where $\mu = m_C m_X / (m_C + m_X)$ is the *reduced mass*, k the *strength constant* of the bond, and c the light speed in vacuum. Table 6 shows the fundamental wavelengths of the vibration modes for the typical bonds in the POF polymers [28].

As the vibrational absorption of the groups C—X is more intense for the first harmonics (specifically, the intensities of such absorption peaks decrease one order of magnitude when the order of the harmonic diminishes in one unity), this phenomenon explains the high attenuation of POFs in the infrared and red spectrum regions [29]. In addition, this behavior suggests a way to improve the POF transparency: by replacing the atoms of hydrogen by heavier elements; the vibrations shift toward longer wavelengths, so the influence of the vibrational absorption in the visible and the infrared frequencies (for which Rayleigh dispersion is also lower) becomes negligible. Taking this fact into account, some PMMA POFs have been deuterated (PMMA-d8), which has yielded attenuations on the order of 10 dB/km [2]. However, the price of deuterium makes this type of POFs prohibitive. Another problem of the PMMA-d8 core POF is the ease of which it absorbs humidity in the polymer. This humidity would increase the attenuation significantly as a result of the strong vibrational absorption of the groups O—H, especially in the near infrared region.

To suppress water vapor absorption, the solution adopted five years ago is fluorine substitution for hydrogen in the core polymer. With such POFs (Lucina), values on the order of 16 dB/km have been achieved nowadays [30]. In addition, fluorinated polymers prevent the penetration of moisture into the polymer, in contrast to deuterated ones. Another advantage is that fluorinated POFs can be

TABLE 6
Experimental Results Yielding the Wavelengths for the Fundamental Vibrations of the Bonds C—X (μm)

Bond C—H	3.3–3.5
Bond C—D	4.4
Bond C—F	8.0
Bond C—Cl	11.7–18.2
Bond C—O	7.9–10.0
Bond C—C	7.9–10.0
Bond C=O	5.3–6.5
Bond O—H	2.8

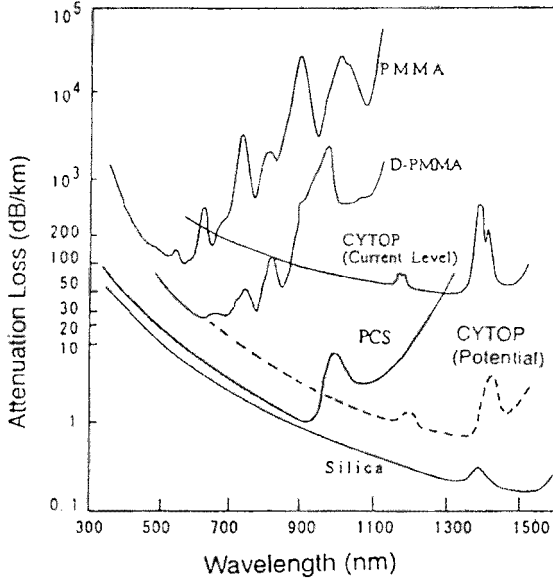


FIG. 7. Transmission loss spectra for various fibers: PMMA, D-PMMA (deuterated), CYTOP, PCS, and silica. The data correspond to those presented in 1996 (from [3]).

utilized for any wavelengths between 850 and 1330 nm, since their attenuation in this range remains below 40 dB/km (Fig. 7) [31]. Moreover, these new POFs can be used with the emitters and receivers designed for glass optical fibers.

On the other hand, polymers, as all organic materials, absorb light in the ultraviolet spectrum region. The mechanism for this absorption depends on the electronic transitions between energy levels in the molecular bonds of the material. The absorption of a photon causes a transition toward higher energy levels; specifically, the light absorbed serves to complete the transitions $n \rightarrow \pi^*$ of the double bonds carbon-carbon $>C=C<$ and the transitions $\pi \rightarrow \pi^*$ of the carbonyl groups $>C=O$ [29]. Generally, the electronic transition absorption peaks appear at wavelengths in the ultraviolet region, and their absorption tails have an influence on the POF transmission loss. According to *Urbach's rule*, the attenuation coefficient due to electronic transitions in PMMA and in PS is given by [29]:

$$\alpha_e(\text{PMMA}) = 1.58 \cdot 10^{-12} \exp\left(\frac{1.15 \times 10^4}{\lambda}\right) \quad (8)$$

$$\alpha_e(\text{PS}) = 1.10 \cdot 10^{-5} \exp\left(\frac{8 \times 10^3}{\lambda}\right).$$

In addition, there is another type of intrinsic loss, caused by fluctuations in the density, orientation, and composition of the material, which is known as *Rayleigh scattering*. The density fluctuations (thermal excitation of compressional modes) depend on the compressibility $\beta|_T$ and on $\frac{\partial \varepsilon}{\partial \rho}|_T$, where ε , ρ , and T are, respectively, the dielectric constant, the density, and the temperature. The orientation fluctua-

tions are caused by the anisotropy of the monomers and by the crystallinity of the polymeric links. Finally, the composition fluctuations arise from the addition of substances to achieve the desired refractive index profiles (in the case of GI POFs). These three effects modify the refractive index in distances on the order of the wavelength. This phenomenon gives rise to an absorption coefficient α_R that is inversely proportional to the fourth power of the wavelength, i.e., the shorter is λ the higher the losses are. For a PMMA POF we have that α_R is given by [12]:

$$\alpha_R(\text{PMMA}) = 13 \left(\frac{633}{\lambda} \right)^4. \quad (9)$$

The scattering process can be interpreted physically in a very easy manner. Let us imagine that a ray traveling through the fiber finds a microscopic variation in the refractive index. Such a variation gives rise to the refraction and reflection phenomena and the incident ray scatters in all directions. As not all the directions correspond to guided rays, part of the light power is lost by radiation. Even if the new ray direction corresponds to a guided one, the sense of the propagating ray can be reversed.

If we add the contributions to the attenuation due to the absorption caused by molecular vibrations, electronic transitions, and Rayleigh scattering, we obtain the ultimate transmission loss limit to which we approach as the manufacturing process improves [30, 32]. Table 7 shows the various loss factors and the theoretical attenuation limits for PMMA, PS, and CYTOP (Lucina) POFs, respectively [2, 30–32].

2.5.2. Extrinsic Losses

There also exists an extrinsic absorption caused by impurities in the core of the POF, fundamentally originated by the presence of transition metal ions (nickel, cobalt, chromium, manganese, iron) and the hydroxyl group (OH^- , although the most significant extrinsic losses are, generally, those arising from the dispersion due to structural imperfections in the POF, generated during the manufacturing process [2]. As can be seen in Table 7, these losses are equal to 4 dB/km in the

TABLE 7
Loss Factors and Theoretical Attenuation Limits for POFs with Different Cores

Loss factor (dB/km)	PMMA (568 nm)	PS (672 nm)	CYTOP (1300 nm)
Total loss	55	114	16
Absorption	17	26	10
Rayleigh dispersion	18	43	2
Structural imperfections	20	45	4
Theoretical attenuation	35	69	12

best case, which is a rather high value in comparison with that of conventional optical fibers, whose corresponding losses are lower than 0.1 dB/km [33].

The future success of POFs depends on the developments in the manufacturing process toward an improvement in their transparency. In the next section we will discuss one of the main sources of extrinsic losses.

2.5.2.1. Absorption by impurities. During the manufacturing process the POF can absorb some contaminants. The presence of these impurities is unavoidable, so they are always a cause of light absorption. Some transition metal ions provoke a higher attenuation than others, but most of them have absorption bands in the visible and near infrared region of the optical spectrum. Table 8 shows the loss caused by typical metallic impurities [34, 35]. The most dangerous metal ions are Co ions, which increase the attenuation in 10 dB/km for concentrations of 2 ppb. Impurities other than those shown in Table 8 are not frequently found in POFs, so they have little influence on POFs' absorption losses.

From Table 8 we can note that hydroxyl groups (OH^-) originate an important increase in absorption, especially in the infrared region, the cause being the water absorbed during and after the manufacturing process. In general, these impurities present a fundamental vibrational absorption frequency whose high harmonics lie in the visible and infrared regions of the spectrum. On the other hand, fluoropolymers do not absorb water easily, so attenuation due to water absorption in fluorinated POFs, such as CYTOP POFs, is negligible.

2.5.2.2. Radiation losses. When an optical fiber is bent, an excess of attenuation appears, due to radiation losses. Fibers can be subjected to two types of bends. When talking about bends of appreciable dimensions as, for example, those produced when rolling the fiber on a reel, we call them *macrobends*. On the contrary, when bends refer to small-scale fluctuations in the fiber axis (on the order of the fiber diameter, as in Fig. 8), we call them *microbends*. These are caused either by defects in the manufacturing of the fiber or by nonuniform lateral pressures generated during the cabling process. The losses arising from both types of bends can be utilized for the design of POF-based sensors, although most times

TABLE 8
Loss Induced by Contaminants

Metal ion	Concentration (ppb)	Loss (dB/km)
Co	2	10 (visible)
Cr	1	1 (650 nm)
Fe	1	0.7 (1100 nm)
Cu	1	0.4 (850 nm)
OH^-	1	50 (1380 nm) 2.4 (1130 nm) 1 (950 nm)

Note: ppb means 1 impurity atom per 10^9 atoms.

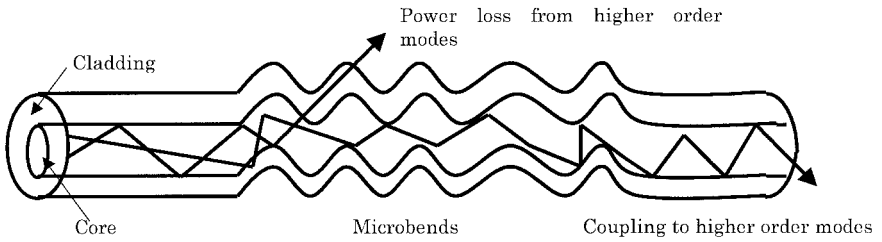


FIG. 8. POF radiation losses induced by microbends.

the goal is to minimize these losses by means of a careful manufacture and installation.

Macrobends are mainly produced during the POF installation process. When the curvature is small, losses are practically negligible. As the bend radius decreases radiation losses increase, the losses being higher for GIPOFs than for SIPOFs of the same diameter. For example, the total radiation loss caused by a full turn in a typical PMMA SIPOF of 1 mm diameter is shown in Fig. 9a for different bend radii. The power decay when reducing the bend radius is exponential, with an exponent that depends on various parameters such as ϑ_c , R , a , n_{co} , and λ . The mechanism by which these losses arise is shown in Fig. 9b [15].

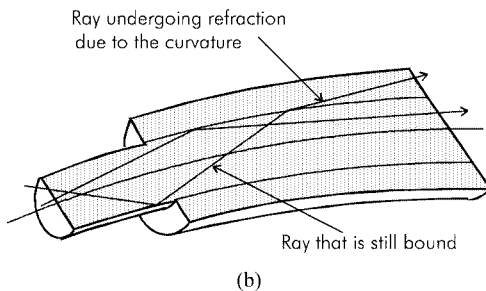
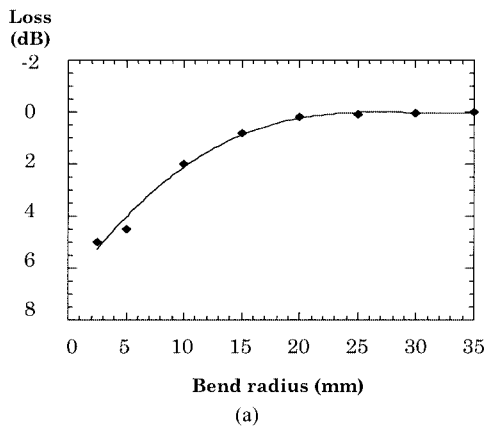


FIG. 9. Radiation losses in a SIPOF induced by macrobends. (a) Experimental results for a PMMA POF with a core radius of 0.49 mm. (b) Mechanism responsible for bending losses.

2.5.2.3. Waveguide imperfections. Waveguide geometrical and structural imperfections comprise changes in the diameter, eccentricity, ellipticity, and core index profile, as well as bubbles, cracks, dust in the core or cladding, and defects at the core–cladding interface. These imperfections provoke a total scattering loss that is roughly independent from the wavelength, so they can be taken into account by adding a constant loss contribution. This is typically about 4 dB/km at 1300 nm for the best quality CYTOP and 20 dB/km for a PMMA POF at 680 nm.

The aforementioned imperfections are formed during the POF manufacturing process. Figure 10 shows the effect that slight nonuniformities in the POF’s radius and in the refractive index of the core have on the power losses. These results correspond to the case of slowly varying SI POFs with small-amplitude nonuniformities, i.e., when the variation of the fiber parameters is negligible for propagation distances on the order of the ray half period.

Considering small amplitude variations in the core radius, the amount of radiated power P_{rad} relative to the input bound power P_{br} can be calculated as [15]

$$\frac{P_{rad}}{P_{br}} = 1 - \frac{a^2(z)}{a^2(0)}, \quad (10)$$

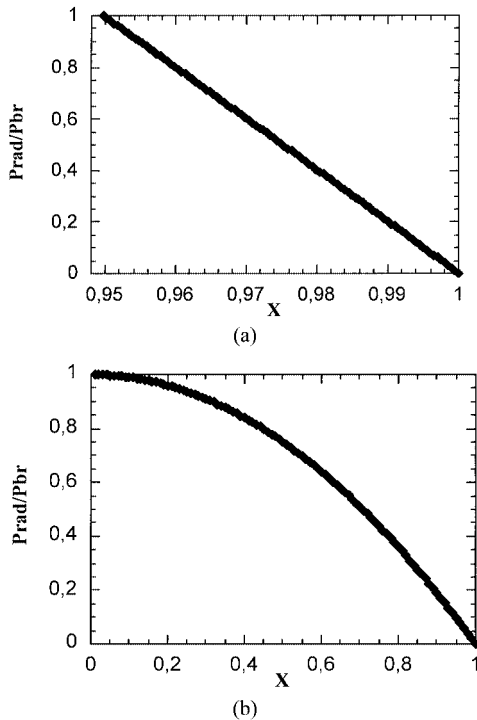


FIG. 10. Power loss originated by small radius variations (a) and by small core refractive index variations (b) along the propagation direction in a PMMA-based SIPOF; $n_{co}(0) = 1.492$, $n_{cl} = 1.417$.

where $a(z)$ is the core radius at a certain position z along the POF. Similarly, the amount of radiated power due to small refractive index variations is

$$\frac{P_{rad}}{P_{br}} = 1 - \frac{x^2 - \frac{n_{cl}^2}{n_{co}^2(0)}}{1 - \frac{n_{cl}^2}{n_{co}^2(0)}}, \quad (11)$$

where $x = n_{co}(z)/n_{co}(0)$ and $n_{co}(z)$ is the core refractive index at the position z . For the calculations, the cladding refractive index was assumed to be constant. It can be observed in Fig. 10a that, for small variations in the radius (5%), the power lost is around 8%. However, small variations in the core refractive index are much more important: a 1% deviation from the mean value can yield power losses as high as 20% (Fig. 10b).

Another source of power losses comes from the anisotropy of the index of refraction. Pierrejen *et al.* have found structural heterogeneities in PMMA POFs due to the orientation of PMMA chains during the drawing process [36]. Depending on the manufacture method and on the POF, the anisotropy fluctuates between 10^{-4} and 10^{-5} .

2.6. Dispersion and Bandwidth

The majority of fiber optic transmission systems are digital; that is, the information is sent through the fiber in the shape of pulses. A pulse, during its propagation through the fiber, experiences a temporal spread known as *temporal dispersion* or, simply, *dispersion*. The phenomenon is shown in Fig. 11.

Dispersion also affects analogue communications, because it produces a distortion in the waveform of the signal. Therefore, in any communications link through an optical fiber it is observed that the dispersion is the parameter that determines the maximum bandwidth that can be transmitted through the optical fiber. The factors that contribute to the waveform distortion are basically three: *modal dispersion*, also called *intermodal*, *material dispersion*, and *waveguide dispersion*, although these two last types of dispersion can be grouped together with the name *chromatic* or *intramodal dispersion*.

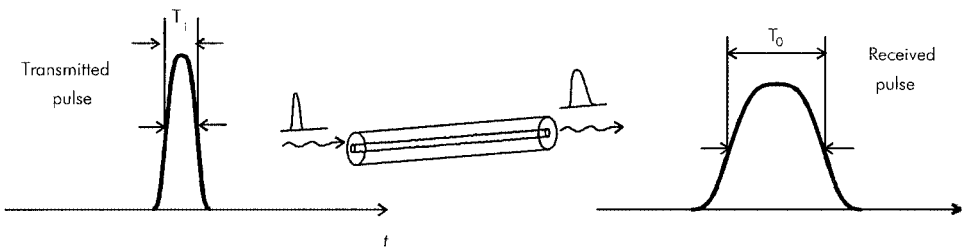


FIG. 11. Temporal dispersion in a POF.

- *Modal dispersion* (σ_m) only affects multimode fibers (as, for example, POFs) and it is caused by the different modes or paths followed by light rays in the fiber, which gives rise to different ray transit times.

- *Material dispersion* (σ_{mat}) arises from the spectral width of the light source $\Delta\lambda$, which is comparatively large in the case of an LED (for example, 25 nm at half height) and small in the case of a laser diode (between 1 and 2 nm) [25]. This type of dispersion occurs because the refractive index of a material is a function of the wavelength, so the different components of the light spectrum travel at different speeds and the pulse broadens.

- *Waveguide dispersion* (σ_{go}) is practically insignificant with fibers that convey many modes, such as POFs. This dispersion is due to the influence of the wavelength, as compared to the core radius, on the propagation speed of each mode. It is the same kind of dispersion as that observed in metallic microwave waveguides.

With respect to SI POFs, it can be proved that their actual modal dispersion is significantly smaller than that calculated with the model of an ideal fiber without mode mixing, i.e., when considering the theoretical time delay between the fastest and the slowest ray propagating along the fiber (at $\theta = 0$ and at $\theta = \theta_c$, respectively) [37]. This fact is explained by the irregularities and inhomogeneities existent in the fiber, which produce a strong interchange of energy between adjacent modes [38]. This interchange provokes a considerable redistribution of modes in a short length of fiber, and it contributes to a greater power loss and to a higher bandwidth. The length for which the interchange of modes is complete is called *equilibrium* or *coupling* length L_{co} , and the modal distribution for such a distance is known as *equilibrium modal distribution* (EMD). Figure 12 shows the results obtained by Jiang *et al.* [38] for a step-index POF. As can be seen from these results, the equilibrium is reached for distances around 15 m when the numerical aperture is large. If this is small, then the equilibrium is reached much later. The coupling length is much smaller than that observed with conventional fibers, for which L_{co} is of the order of several kilometers [39]. This seems to be related to the large number of rays involved in the propagation of light along POFs as well as to the large number of structural imperfections, mainly at the core-cladding interface.

The dispersion σ stands for the root-mean-square width of the output pulse when an input pulse of negligible duration covers a certain length of optical fiber. It can be calculated from the following equation [33]:

$$\sigma^2 = \sigma_m^2 + (\sigma_{mat} + \sigma_{go})^2 \approx \sigma_m^2 + \sigma_{mat}^2. \quad (12)$$

To calculate the modal dispersion of meridional rays in a step-index POF, we must take into account that the rays parallel to the fiber symmetry axis are the fastest ones, as indicated in Fig. 13.

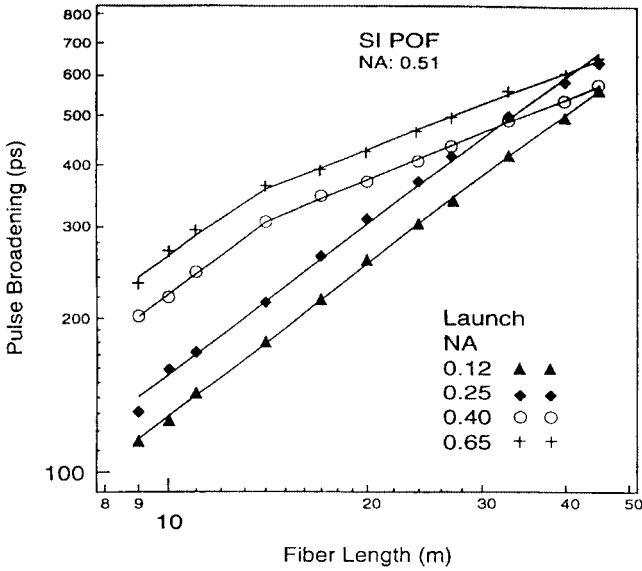


FIG. 12. Logarithmic representation of the modal spread in a SI POF as a function of the fiber length, taking the launch numerical aperture as a parameter. The fiber core material is PMMA, the fiber numerical aperture is 0.51, and the fiber diameter is 1 mm (from [38]).

When the ray propagates parallel to the fiber axis, the distance L_0 covered is minimum, whereas this is maximum if the ray makes the complementary critical angle θ_c with the axis. As the distances covered are different, the instants at which the two rays reach the end of the fiber are also different, and the difference in time will be given by:

$$\Delta t = t_2 - t_1 = \frac{n_{co}}{c} L_0 \left(\frac{1}{\sin \theta_c} - 1 \right). \quad (13)$$

The modal dispersion depends on the capacity of the fiber to accept light coming from the light source (Fig. 14). When coupling the light emitted by the source into the optical fiber, light rays coming from the source are refracted, passing from the air to the fiber core. In this process, the ray trajectories and angles vary. Once inside the core, only those rays making an angle smaller than the complementary critical one with the symmetry axis will be bound. Therefore, the capacity of a fiber

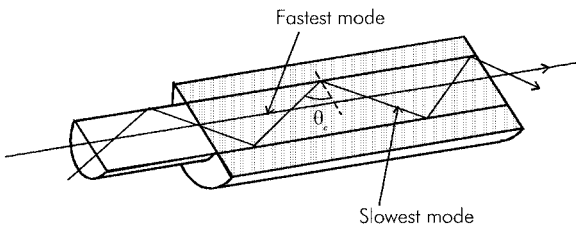


FIG. 13. Trajectories of the slowest and the fastest ray in a step-index POF.

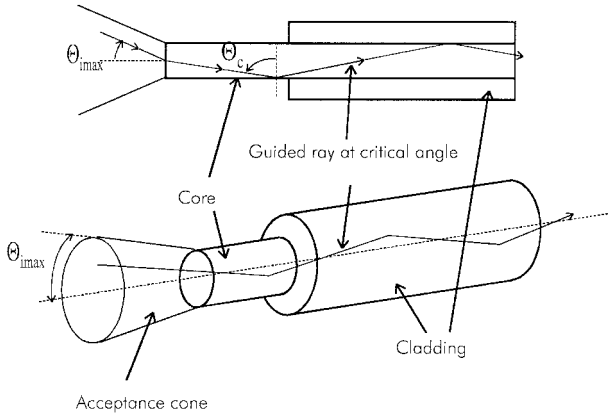


FIG. 14. Definition of the numerical aperture in a step-index POF.

to capture light energy depends on the angle of aperture of the *admission cone*, which is the cone containing all the possible ray directions in the air for rays to be bound when they enter the fiber. The sine of the angle of aperture of this cone is called the NA, and it is given by:

$$NA = \sin \theta_{imax} = \sqrt{n_{co}^2 - n_{cl}^2}. \quad (14)$$

The NA is a very important parameter of optical fibers, since it indicates their capacity for accepting and guiding light. Those fibers with a higher numerical aperture can accept more light. The numerical aperture of a typical POF is very large in relation to glass fibers, approximately 0.5, which facilitates the coupling of light into the fiber. There are also POFs with a reduced numerical aperture, which are used to achieve higher transmission speeds [12]. The lower the numerical aperture, the higher the bandwidth is, because the modal dispersion decreases, since fewer modes will propagate through the fiber. With regard to the emitters and detectors, these also have their numerical aperture, depending on the emission and reception angles. It is especially important to match the numerical apertures of the optical fiber and the light source, so as to couple the emission power into the fiber efficiently.

In a graded-index POF, the refractive index decreases as we separate from the fiber symmetry axis, according to Eq. (1), so those rays that cross the symmetry axis with greater angles are also faster, which compensates for the differences in distance covered [40]. The expression for the modal dispersion obtained from the WKB method is [41]

$$\sigma_m = \frac{LN_1\Delta}{2c} \frac{g}{g+1} \left(\frac{g+2}{3g+2} \right)^{1/2} \times \left[C_1^2 + \frac{4C_1C_2\Delta(g+1)}{2g+1} + \frac{4\Delta^2C_2^2(2g+2)^2}{(5g+2)(3g+2)} \right]^{1/2}, \quad (15)$$

where

$$C_1 = \frac{g - 2 - \varepsilon}{g + 2}; C_2 = \frac{3g - 2 - 2\varepsilon}{2(g + 2)}; \varepsilon = \frac{-2n_{co}}{N_1} \frac{\lambda}{\Delta} \frac{d\Delta}{d\lambda};$$

$$N_1 = n_{co} - \lambda \frac{dn_{co}}{d\lambda}; \Delta = \frac{n_{co}^2 - n_{cl}^2}{2n_{co}^2}.$$

In Fig. 15 we show the variation of the modal dispersion as a function of the profile exponent g . The optimum value for g is slightly lower than 2; specifically $g = 1.97$ [42].

To calculate an expression for the material dispersion, we must consider the emission spectrum of light sources. This spectrum can depend on parameters such as temperature, and it extends into a range of wavelengths $\Delta\lambda$ located around a central wavelength. Therefore, the material dispersion depends on the temperature, because $\Delta\lambda = \Delta\lambda(T)$.

As the refractive index of the core's constituent materials in a POF depends on the wavelength, the power components corresponding to different wavelengths travel at different speeds. The components representing the shortest wavelengths see a higher refractive index and travel more slowly than those representing longer wavelengths (see Fig. 16a) [43]. The global effect gives rise to pulse broadening, since the output pulse is composed of all wavelengths and these undergo different delays. The effect occurs within each mode or ray.

Figure 16b also shows the *material dispersion coefficient* $M(\lambda)(ns/km \cdot nm)$, which yields the pulse broadening per unit length and per unit wavelength. It is defined as $M(\lambda) = -\frac{\lambda}{c} \frac{d^2n}{d\lambda^2}$. The material dispersion is given by the relative delay

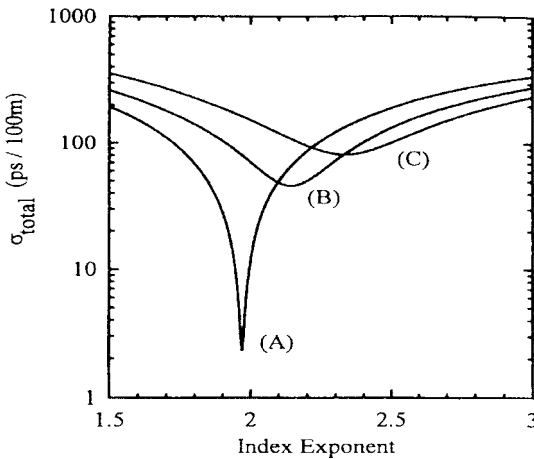


FIG. 15. Dispersion σ versus the exponent g in a PMMA-core GI POF, for a light source spectral width of 2 nm. (a) Only modal dispersion is considered. (b) Both modal and material dispersion are considered for $\lambda = 780$ nm. (c) Both modal and material dispersion are considered for $\lambda = 650$ nm (from [40]).

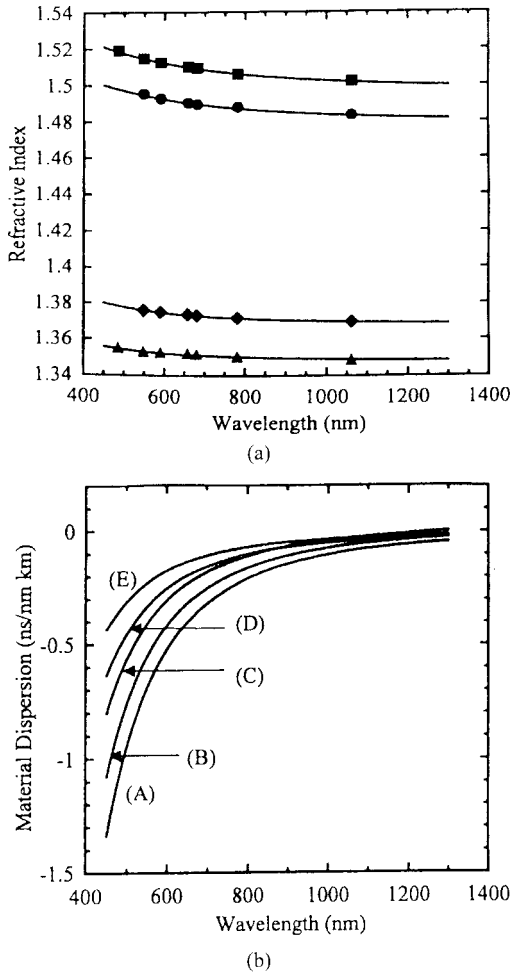


FIG. 16. (a) Dependence of the refractive index on the wavelength for several polymers utilized in the manufacture of a GI POF core (■, BEN-doped PMMA; ●, PMMA, DBP-doped PHFIP-2FA; ▲, PHFIP-2FA). (b) Material dispersion for several polymers utilized for this purpose. ((A) BEN-doped PMMA, (B) PMMA, (C) silica, (D) DBP-doped PHFIP-2FA, (E) PHFIP-2FA) (from [40]).

of the pulse component corresponding to the shortest wavelength ($\lambda - \Delta\lambda/2$) referred to the component corresponding to the longest wavelength ($\lambda + \Delta\lambda/2$), provided that both components belong to the same mode. This dispersion is obtained by the following expression [40, 43];

$$\sigma_{mat} = \frac{L\Delta\lambda}{\lambda} \left[\left(\lambda \frac{d^2 n_{co}}{d\lambda^2} \right)^{1/2} - 2\lambda^2 N_1 \Delta \frac{2C_1 \alpha}{2\alpha + 2} \frac{d^2 n_{co}}{d\lambda^2} + (N_1 \Delta)^2 \left(\frac{\alpha - 2 - \varepsilon}{\alpha + 2} \right)^2 \frac{2\alpha}{3\alpha + 2} \right]^{1/2}, \quad (16)$$

where $\Delta\lambda$ is the root mean square of the light source spectrum width.

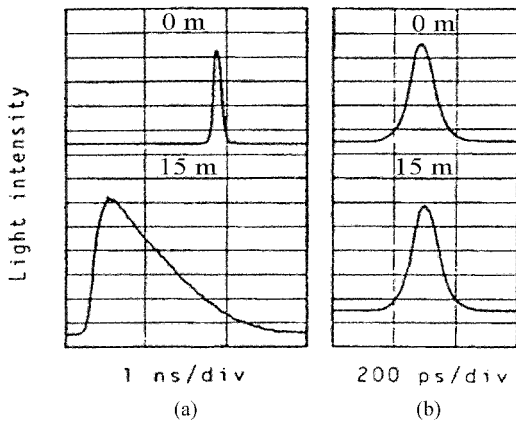


FIG. 17. Comparison between the input and output pulses for a 15 m long PMMA POF: (a) step-index POF and (b) graded-index POF (from [18]).

Figure 17 shows the broadening of a light pulse emitted by a 670 nm laser diode when it travels along 15 m of a step-index PMMA POF (a) and along a graded-index POF of similar composition (b).

For the sake of comparison between the importance of the chromatic dispersion and that of the modal one in a short length of a step-index POF, we will mention that measurements carried out with 24 m of PMMA POF, with numerical aperture 0.47, revealed that the chromatic dispersion arising from the LED spectrum width limited the bandwidth to 1 GHz, which was less than the 2 GHz imposed by the modal dispersion. This fact was due to the strong mode conversion caused by inhomogeneities in the fiber's core, as can be partially explained from Gloge's diffusion equation [44].

We end this section by showing, in Fig. 18, the dispersion obtained experimentally and theoretically for a perfluorinated GIPOF. As can be observed in the

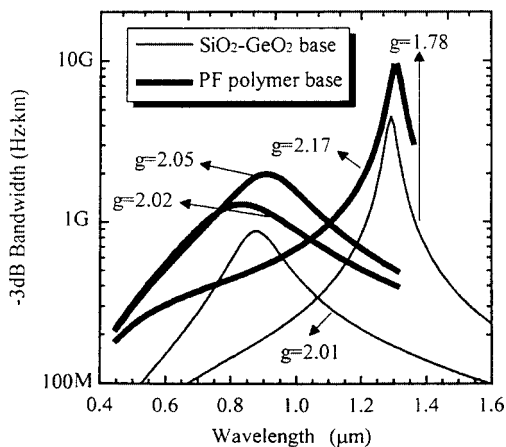


FIG. 18. Dependence on the wavelength of the product bandwidth*distance for a perfluorinated GI POF and for a multimode $\text{GeO}_2\text{-SiO}_2$ graded-index optical fiber (from [26]).

figure, these fibers allow products $bandwidth \cdot distance$ on the order of 10 GHz \cdot km to be achieved for a profile exponent $g = 1.78$ and $\lambda = 1.3 \mu\text{m}$ [26, 40]. A disagreement between measured and estimated bandwidth can be seen. At the beginning, this difference was attributed to mode coupling effects. However, recent studies have demonstrated that mode coupling in GIPOF is very small and that the differential mode attenuation is responsible for this disagreement. In GIPOFs, the attenuation increases when the mode number increases. From measurements of differential mode attenuation, the bandwidth characteristics can be successfully explained and predicted [45].

2.7. Mechanical Properties

Several authors have studied the mechanical properties of POFs. Most of these studies have been focused on the attenuation induced by bends and tensile or torsion stresses [23, 46–49]. In contrast to glass fibers, POFs are made of plastic materials. Another difference is that Young's modulus for a POF is nearly two orders of magnitude lower than that of a silica fiber (2.1 Gpa for a PMMA POF) [46]. For this reason, even a 1 mm diameter POF is sufficiently flexible to be installed according to typical fiber configurations. For the same reason, the minimum bend radius for POFs is smaller, since plastic is more ductile and much less stiff than silica. Similar results have been obtained for polycarbonate POFs, for which Young's modulus lies in the range between 1.55 and 2.55 Gpa [47].

As for the transmission rate through a POF, this also depends on some mechanical properties [47]. For example, if the POF is elongated the 10% of its length, the attenuation increases less than 0.1 dB. Regarding other factors that can change the POF's optical properties, cyclic bendings can also cause variations in the attenuation, up to a certain limit (< 0.15 dB for 1000 bending times with a bend radius of 50 mm, in the case of 1 mm PMMA POFs) [23, 50].

2.8. Thermal Properties

As POFs are made of polymer, they can operate at temperatures up to 80–100°C. Above this limit, POFs begin to lose their rigidity and transparency. The operation temperature can be increased up to 125°C or even to 135°C by using a jacket made of crosslinked polyethylene or of a polyolefine elastomer [2–12, 22, 23].

On the other hand, the resistance of POFs to high temperatures strongly depends on the degree of moisture. For example, if the POF is maintained at 85°C with 85% of relative humidity for 1000 h, the attenuation will increase in 0.02 dB/km. If the relative humidity level is around 90%, the attenuation increases more than 0.03 dB/m [50]. This behavior is due to the strong OH^- absorption band in the visible range. Fluorinated fibers do not absorb water, so the attenuation rate through them is not altered significantly by the degree of moisture [7, 51].

High bandwidth GIPOFs also have a high thermal stability. No distortion in bandwidth is observed even after more than 10,000 h of aging at 85°C [52].

2.9. Chemical Resistance

Most of the work on POFs' chemical resistance deals with the behavior of POFs when they are in contact with those liquids typically found in cars. For example, polycarbonate POFs without jacket only resist 5 min immersed in 85-octane petrol. However, these POFs are able to withstand oil and battery liquid for a long time [53]. The polyethylene jacket of a fiber cord serves to protect the POF when it is dipped into chemical products. When using this jacket, PMMA POFs are protected against liquids such as water, NaOH, sulfuric acid (34.6%), or engine oil. In any of such liquids, the attenuation remains constant when the coated POF is dipped into the liquid at 50°C for 1000 h. [54].

Fluorinated POFs (CYTOP), do not show changes in their attenuation when they have been dipped for 1 week into chemical acids such as 50% HF, 44% NaOH, and 98% H₂SO₄ or organic solvents such as benzene, hexane, MEK, and CCL₄ [51].

3. PROSPECTS AND FUTURE OF POFs

3.1. Polymer Optical Fiber Amplifiers

In 1993, researches in Japan demonstrated the first polymer optical fiber amplifier (POFA) employing a PMMA-based GIPOF [55]. Specifically, Tagaya *et al.* doped the PMMA POF with organic dyes. They chose Rhodamine B because of its high fluorescence in the visible range and its high photochemical stability. By using a 0.5 m long 0.25 mm-core-diameter POFA they observed a high gain of 27 dB at 591 nm with a Rhodamine B concentration of 10 ppm. In their experiment they utilized a 620 W pump source centered at 532 nm. The conversion efficiency was better than 60% (420 W of output power for a 0.85 W input signal). Since then several improvements have been realized [56–58].

Kuriki *et al.* demonstrated efficient and photostable laser action in a GIPOF doped with Rhodamine B and other organic dyes such as perylenes and pyrromethanes [59]. The laser wavelength was in the range between 583 and 640 nm and the fibers used were 5 cm long and 0.7 mm in diameter. The pump power was 640 W and it was centered at 532 nm. As usual in this kind of amplifier, the signal gain depended on the power-pump signal. Figure 19 shows this dependence for a Rhodamine B doped GI POF.

Peng *et al.* achieved a high amplification by using an SI POF doped with Rhodamine B in a proportion of 2500 ppm., as well as a tuneable wavelength from 610 to 640 nm [58]. They obtained signal gains of 21 and 15 dB for wavelengths of 620 and 635 nm, respectively, utilizing a 950 W 532 nm input pump power and a pulse width of 5 ns at 532 nm. The importance of these results lies in the fact that the amplification occurs at wavelengths close to the most used transmission window of PMMA POFs. Similarly, Tagaya *et al.* obtained a signal gain of about 18 dB at 649 nm by using a long GI POF and an organic dye called 04PC. The pump power was on the order of 1 KW [56].

In spite of these discoveries, researchers still have a long way to cover before POFAs begin to be used, as has happened with single mode POFs. The reason is

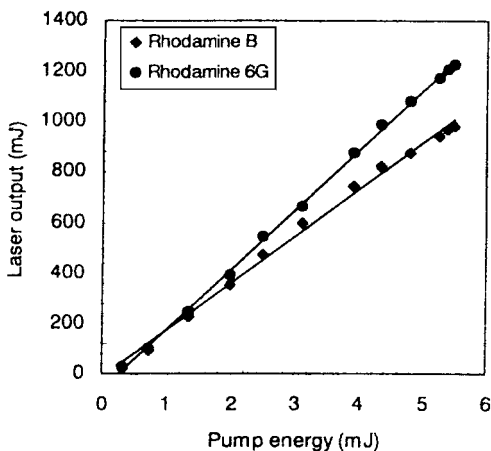


FIG. 19. Input–output curves for the Rhodamine 6G and the Rhodamine B-doped polymer fibers (from [59]).

that this type of amplifier requires the use of high power pump sources, which removes the most important advantage of POFs, that is to say, their low price.

3.2. Scintillating Plastic Optical Fibers

Several research groups have developed scintillating polymer optical fibers (SPOFs), mainly the French Commissariat à l'Énergie Atomique [59] at the beginning of 1980. SPOFs are insensitive to electromagnetic fields and they present a good physical resistance to radiation. For both reasons they are particularly valuable in high-energy-physics sets of equipment. Generally, SPOFs are doped PS fibers with a cladding of PMMA. Their emission peak ranges from 428 to 538 nm [9], depending on the dye used to dope the POF and on its concentration. SPOFs have application in the field of high energy physics as components of track detectors, high-resolution spatial detectors, and particle energy meters [9, 60].

3.3. Multicore Plastic Optical Fibers

The multicore plastic optical fiber (MCPOF) is one single fiber composed of many small cores arranged like islands in a sea of cladding (Fig. 3). The cores may be surrounded by a first cladding in order to reduce bending losses. For instance, a 0.25 NA MCPOF with 37 cores and a total outer diameter of 130 μm , wound around a 3 mm-radius stick, yields 0 dB of bending loss [61].

3.4. Local Area Networks

Despite the high number of present and future applications of POFs, LAN networks constitute a unique opportunity, at least from the economic point of view. More specifically, the great opportunity of POFs consists in using them as the transmission medium for domestic communications networks. Since the creation of

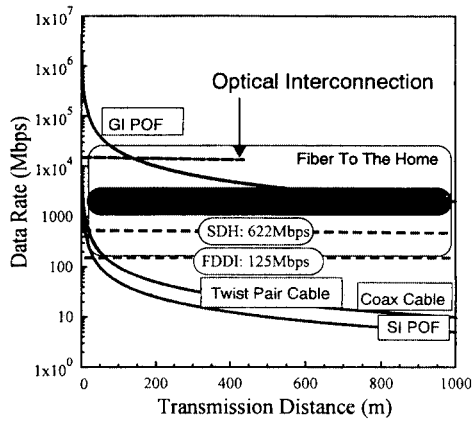


FIG. 20. Different application areas of POF and of the alternative transmission media (from [26]).

the standard 1394 by Apple Computer, orientated toward the connection of different domestic sets of equipment [62, 63], POF technology has tried to find its main application in this field. Nowadays, POFs constitute the most suitable transmission media in the aforementioned field, since they present bandwidths in the range between 1 and 10 Gbs*km, which are much higher than those of twisted pair, and also because POFs have a lower price and better prospects of improvement in their technical characteristics. In addition, when compared with conventional optical fibers, the price and simplicity of POF technology relegate conventional fibers to a second plane in domestic networks. Figure 20 serves to compare the capabilities of all of these transmission media as a function of the distance and the bandwidth.

It is hoped that, in the near future, POFs will experience a market explosion based on the widespread deployment of the fiber to the home (FTTH) and even in the home. If this is the situation, the POF market will expand in the way shown in Fig. 21, growing from \$8 million this year to \$250 million in 2008 [64].

This spectacular growth will be led by telecommunication applications (50% growth in high speed data transmission) and vehicle applications (32% growth in on-board POF networks and car lights and gauges). The rest of the market will be dedicated to computer applications, lighting, and industrial applications.

In the next 10 years we also hope to have home wiring according to the standard 1394 [63], similar to that shown in Fig. 22. If the perfluorinated fibers prevail in the market, then they will offer the advantage of allowing us to use the same wavelength as that of the signal reaching our homes (1300 nm).

3.5. POF-Based Sensors

Although many of the applications of optical fibers are based on their capacity to transmit optical signals with low losses, it can also be desirable for the optical fiber to be strongly affected by a certain physical parameter of the environment. In this

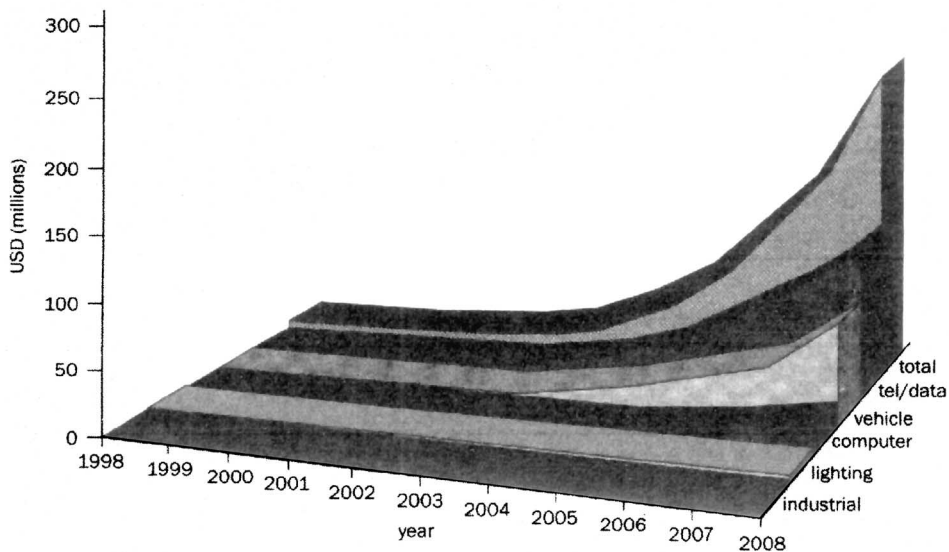


FIG. 21. Ten year forecast for POF by industry sector (from [64]).

way, it can be used as a sensor of such a parameter. In this section we describe some sensors based on the light power radiated by an optical fiber.

There are many strong arguments for the use of POFs as sensors. In addition to their easiness to handle and low price, they present the advantages common to all

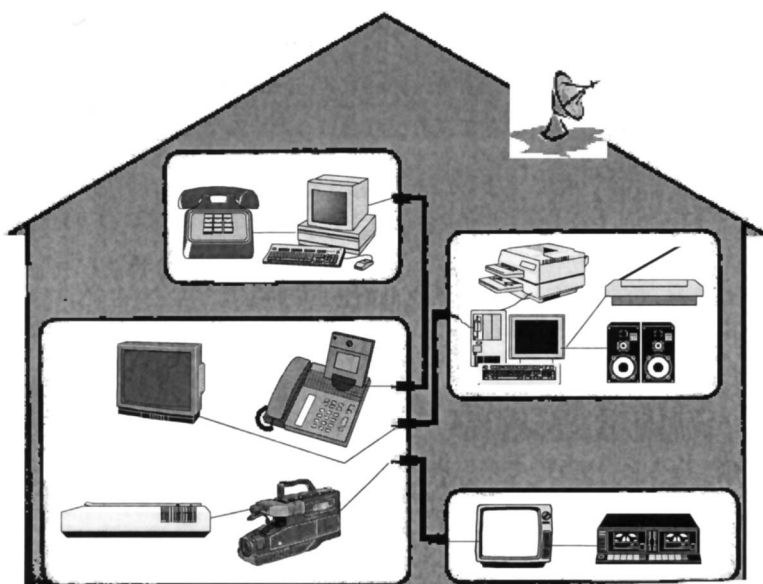


FIG. 22. Aspect of a house cabled with POF following the standard IEEE 1394.

multimode optical fibers. Specifically, we can mention that the flexibility and small size of optical fibers enable a great sensitivity to be achieved without having to occupy a big volume. Moreover, it has been proved that a POF can be employed to detect a great variety of parameters, including temperature, humidity, pressure, presence of organic and inorganic compounds, wind speed, and refractive index. On the other hand, POF-based optical sensors eliminate the risk of electric sparks in explosive environments, and they can be read from remote positions.

The mechanisms allowing us to detect a physical parameter by using POFs are very diverse, although most of them are based on light intensity modulation. Table 9 summarizes some of the most important kinds of POF-based sensors proposed until now [66–100].

TABLE 9
Summary of Some of the POF-based Sensors

Reference	Measurand	Description
[66, 69]	Nuclear radiation	Scintillating POF's convert nuclear radiation into blue light;
[81]		Dye-doped PS, PMMA, or polymethylphenylsiloxane core POFs. POF-based scintillation counter used for the detection of energetic beta particles from radionuclides.
[82]		POFs are used as active materials, which propagate the Cerenkov light created when secondary particles cross them toward photodetectors.
[66]	Sparks	Electric perturbations excite fluorescent fibers
[67]	X-ray	Fluorescent POFs glued to a scintillating plate
[73, 80]		Sensor based on fluorescent POFs. The POF core is doped with organic fluor, while a double cladding contains an inorganic product (ZnS) to convert X-ray energy into visible light (blue-green).
[68]	pH	Porous POFs; pH indicators are copolymerized with a hydrophilic polymer system. Sensor transit time can be tailored by adjusting the composition and properties of the polymer.
[88]		pH sensor in the range 1.0–8.0 (0.05 pH units accuracy), suitable for gastro-oesophageal applications.
[91]		Two different acid–base indicators are immobilized at the tip of plastic fibers.
		POF-based sensor with a pencil-shaped distal tip probe, which consists of two POF ends that come together at a common tip. This leads to higher fluorescence detection efficiency.
[68]	Carbon monoxide	Palladium chloride served as the colorimetric reagent and was dissolved into the monomer solution used to make the POF.
[96]	Oxygen	The sensor head consists of a POF with a tetraphenylporphine dye-doped polymer clad on the ARTON core fiber. The POF was pumped by a He–Cd blue laser. Depending on the oxygen concentration the fluorescence is enhanced.
[68]	Ammonia	Porous POFs; pH indicators are copolymerized with a hydrophobic polymer system. The porous polymer is gas permeable but water and ion impermeable. Ammonia changes the pH to a higher value.

TABLE 9—Continued

Reference	Measurand	Description
[70]	Humidity	Based on a fluorescent POF ($L = 3.5$ cm) with a cladding doped with dye molecules that experiment an ionization reaction when water vapor is present.
[87]		Dual-POF amplitude-modulation extrinsic-reflectance sensor to detect changes in water uptake by plant roots and to monitor relative humidity.
[71, 78]	Temperature	A simple thermodetector using a thermosensing discoloration material (TSDM), whose detector is capable of visually discriminating temperature rise by discoloration of the material. It works at 80°C.
[72]		Another design uses polymer blends. The optical transmittance decreases immediately with a temperature rise. It works between 60 and 200°C.
[99]		This sensor is based on the relative temperature intensity of the fluorescence lifetime of Ruby and Cr^{3+} doped materials situated between two POFs.
[74]	Thickness	Novel construction of a dual amplitude-modulating displacement transducer using POFs to measure leaf thickness. Responsivities as high as 11800 V/m with a SNR of 68 dB can be obtained.
[75]	Remote location	POF delivers light from an LED to a remote location. The light is conditioned and shaped into a uniform planar profile. Objects passing through the sensing area interrupt the beam and generate a signal.
[76]	Gas concentration	In POFs with a rhodamine B dye/silicone coating exposed to alcohol gas, the absorption spectrum of dyes changes according to the gas concentration (methanol). It can be used for distributed sensing.
[77]	Chemosensor	Consists in a polymer optical waveguide covered with an ion-selective optical cladding. Chemical recognition transduction into an optical signal is carried out by polymer bound chromoionophores.
[79]	Displacement	Linear displacement POF-based sensor, usable between 15 and 80 mm.
[89]		POF displacement sensor based on three POFs (one emitting and the other two receiving). It yields a linear response over a dynamic range of 85 mm with a 1% accuracy.
[83]	Liquid level	The sensor detects the hydrostatic pressure produced by a column of liquid. The pressure moves a diaphragm some distance away from the POF, which is a function of the liquid height.
[84]	Toxicity	The toxicity biosensor used POFs to measure the fluorescence generated when leaving microorganisms in aqueous suspension hydrolyze fluorescein diacetate FDA).
[84]	Particle concentration	Based in the scattering by the particles contained in an aqueous suspension placed between two parallel POFs separated laterally.
[84]	Flow	A strain optical fiber sensor. It consists of a grooved 0.49-mm-core POF section. Light attenuation depends on strain experienced by the POF's surface.

TABLE 9—Continued

Reference	Measurand	Description
[85]	Three color sensor for visible and UV regions	Based on the fluorescence of doped POFs with quite different absorption and emission spectra (depending on the dyes). Temperature and bending have a small influence on the performance on this sensor.
[86]	Refractive index	The principle of this sensor is the light power leakage along tightly bent POFs stripped of their cladding, introducing more than a half turn in the active POF hardly improves the sensor response.
[95]		Based on the power lost by a partially polished POF due to presence of a liquid on the polished side, which makes the bound ray power decrease.
[90]	High temperature superconducting fault current limiters	Makes use of measurements of bubbles and liquid level using a PMMA SI POF. It works under extreme conditions (77 K).
[92, 97]	Gas leakage	A POF is coated with a polyisoprene cladding layer. This material, when immersed in acetone or alkanes, seems to swell and its refractive index changes from 1.52 to 1.46, depending on the acetone concentration. As a result of this process the POF's output power depends on the acetone concentration.
[93]	Radius	There is a dependence between the bending radius and the POF's attenuation.
[93]	Stress	Uses the dependence between the axial stress and the attenuation, which is reproducible for an elongation of not more than 5% of the POF's total stressed length.
[93]	Radial rotation	As the POF attenuation is in direct proportion to the twisting angle; a rotation angle sensor can be realized.
[94]		Based on the rotation of the polarization plane of rays as they travel along the fiber.
[98]	Wind speed	This is a POF-based sensor that consists of two fibers and a rotating device attached to an anemometer. It is able to measure the wind speed in a wind generator.
[100]	Acid concentrations	Concentrations of HF and HCl acids in water are measured in an intensity setup. Variations of light intensity serve to deduce acid concentrations.

4. CONCLUSIONS

POFs' characteristics make them especially suitable for short-haul telecommunications links and sensors. To improve the maximum transmission distance and speed, GI POFs can be used, especially those made from an amorphous fluorinated polymer called CYTOP. In the field of sensors, those based on POFs allow many different parameters to be measured, such as distance, position, shape, color, brightness, opacity, density and turbidity, and fluorescent POFs serve for particle tracking. POFs have also been employed to make optical couplers and switches.

The success of POFs arises from their easiness to use and the fact that POF production techniques have advanced as much as to enable the manufacture of inexpensive high-quality low-loss POFs.

POFs' attenuation depends on the core diameter and on the numerical aperture of the light source. The basic attenuation mechanisms in a POF can be classified into two big groups: *intrinsic* and *extrinsic*. Among the intrinsic losses we have the *absorption* of the constituent material and the *Rayleigh scattering*. Both contributions depend on the composition of the optical fiber and, therefore, they cannot be eliminated. Thus, they determine the ultimate POF attenuation, which is around 12 dB/km for Lucina. On the other hand, extrinsic losses can be avoided, e.g., *radiation losses*, which will occur when bending the POF with a small curvature radius.

The maximum transmission distance through a POF not only depends on the fiber's attenuation, but also depends on the waveform distortion due to *intermodal* and *intramodal dispersion* as well as to the differential mode attenuation. Of the two types of dispersion, the former depends on the POF's numerical aperture and on the POFs index profile, and the latter depends on the light source's spectral width, among other factors. Although those fibers with a higher numerical aperture can accept more light, there are also POFs with a reduced numerical aperture, which are used to achieve higher transmission speeds. In SIPOFs the theoretical intermodal dispersion is very large, but mode conversion caused by inhomogeneities in the fiber's core can reduce this kind of dispersion significantly. For this kind of POFs, the bandwidth is around 15–50 Mbs*km. In commercial GIPOFs (Lucina, the bandwidth–distance product goes up to 569 MHz*km.

On the other hand, as POFs are made of polymer, they cannot usually operate at temperatures higher than 80–100°C. Above this limit, POFs begin to lose their rigidity and transparency. In addition, POFs' properties can change when they are in contact with some chemical products or when they are subjected to mechanical stresses. Consequently, a great research effort is being done on POFs' constituent materials, including the possibility of making commercial POF-based optical amplifiers.

ACKNOWLEDGMENTS

This work is supported by the Departamento de Educación, Universidades e Investigación del Gobierno Vasco under Projects UE-1998-4 and OD2000UN41 and also by the Universidad del País Vasco under Project UPV 147.345-EA 152/98 ZUBIA. The authors thank Unai Irusta for his help to plot some of the figures.

REFERENCES

- [1] A. M. Glass, D. J. DiGiovanni, T. A. Strasser, A. J. Stentz, R. E. Slusher, A. E. White, A. R. Kortan, and B. J. Eggleton, "Advances in fiber optics," *Bell Labs Technol. J.*, January-March, vol. 5, 168 (2000); R. C. Alferness, H. Kogelnik, and T. H. Wood, "The evolution of optical systems," *Bell Labs Technol. J.*, January-March, 188 (2000).

- [2] T. Kaino, "Polymer optical fibers," in *Polymers for Lightwave and Integrated Optics*. Dekker, New York, 1992; E. Nihei, T. Ishigure, N. Tanio, and Y. Koike "Present prospect of graded index plastic optical fiber in telecommunications," *IEICE Trans. Electron.*, vol. E-80-c, 117–122 (1997).
- [3] H. Murofushi, "Low loss perfluorinated POF," in *Proc. Fifth International Conference on Plastic Optical Fibres and Applications-POF'96*, Paris (France), pp. 17–23, 1996.
- [4] T. Nyu, S. Yamazaki, and A. K. Dutta, "Experiments on 156 Mbps-100 m transmission using 650 nm LED and SI POF," in *Proc. Fourth International Conference on Plastic Optical Fibres and Applications-POF'95*, Boston MA, pp. 119–121, 1995.
- [5] K. Numata, S. Furusawa, and S. Mirikura, "Transmission characteristics of 500 Mbs optical link using 650 nm RC-LED and POF," in *Proc. Eighth International Conference on Plastic Optical Fibres and Applications-POF'99*, Chiba (Japan), pp. 74–77, 1999.
- [6] Y. Koike, T. Ishigure, and E. Nihei "High-bandwidth graded index polymer optical fiber," *J. Light. Technol.*, vol. 13, 1475 (1995).
- [7] M. Naritomi, "CYTOP[®] Amorphous Fluoropolymers for low loss POF," in *POF Asia Pacific Forum 1996*, Tokyo (Japan), 1996.
- [8] U. Steiger, "Sensor properties and applications of POFs," in *Proc. Seventh International Conference on Plastic Optical Fibres and Applications-POF'98*, Berlin (Germany), pp. 171–177, 1998; H. Poisel, K. F. Klein, V. Levin, and G. Lohr, "Progress with the FiberOptic Slipring," in *Proc. Sixth International Conference on Plastic Optical Fibres and Applications-POF'97*, Kauai HI, pp. 22–25, 1997.
- [9] Club des Fibres Optiques Plastiques, *Plastic Optical Fibres: Practical Applications*, Wiley, New York, 1997.
- [10] R. J. Bartlett, S. L. Caulder, R. P. Chandy, D. F. Merchant, R. Morgan, and P. Scully, "Plastic optical fibers sensors and devices," in *Proc. Seventh International Conference on Plastic Optical Fibres and Applications-POF'98*, Berlin (Germany), pp. 245–246, 1998.
- [11] A. J. Schilk and T. W. Bowyer, "The use of scintillating plastic optical fibers for the detection of radioactive contamination," in *Proc. Fourth International Conference on Plastic Optical Fibres and Applications-POF'95*, Boston MA, pp. 171–176, 1995.
- [12] High performance plastic fiber optics, ESKA, Mitsubishi Rayon Co. Ltd.
- [13] I. Gagnadre, G. Boutinaud, and J. Marcou, "Distributeur 1 ver 30 pour fibres optiques polymères," *Pure Appl. Opt.*, vol. 2, 441 (1993).
- [14] D. Marcuse, *Theory of Dielectric Waveguides*, pp. 75–80, Academic Press, San Diego, 1974.
- [15] A. W. Snyder and J. D. Love, *Optical Waveguide Theory*, 2nd ed., Chapman and Hall, London, 1983.
- [16] J. Zubia, P. Cortina, J. Arrúe, J. Miskowicz, and G. Durana, "Light polarization in plastic optical fibers," in *Proc. Ninth International Conference on Plastic Optical Fibres and Applications-POF'00*, Boston MA, Poster presentation and postdeadline papers, 2000.
- [17] L. G. Cohen, "Measured attenuation and depolarization of the light transmitted along glass fibers," *Bell Syst. Technol. J.*, January, 23–42 (1971).
- [18] Y. Koike, "High bandwidth and low loss polymer optical fiber," in *Proc. First International Conference on Plastic Optical Fibres and Applications-POF'92*, Paris (France), pp. 15–19, 1992.
- [19] Sentel Technologies, Polymer Optical Fibers Catalogue, 1999.
- [20] S. R. Vigil, Z. Zhou, B. K. Canfield, J. Tostenrude, and M. G. Kuzyk, "Dual core single-mode polymer fiber coupler," *J. Opt. Soc. Am. B*, vol. 15, 895 (1998).
- [21] D. W. Garvey, Q. Li, and M. G. Kuzyk, "Sagnac interferometric intensity-dependent refractive-index measurements of polymer optical fiber," *Opt. Lett.*, 104 (1996).
- [22] Asahi Glass Industries, Ltd., *Plastic Optical Fibers for High-Speed Transmission*, Technical Bulletin (Luminous NC-1000, NMC-1000, PMC-1000).
- [23] Boston Optical Fiber, *Raytela Polymer Optical Fiber Cord*, Toray Industries, "OptiMega and OptiGiga," 2000.

- [24] Fiber Optic and High Speed Integrated Circuit Components Designer's Catalog, Hewlett Packard, 1997.
- [25] Fiber Optics Data Book 1998–1999, Siemens.
- [26] T. Ishigure, E. Nihei, and Y. Koike, "High bandwidth GI POF and mode analysis," in *Proc. Seventh International Conference on Plastic Optical Fibres and Applications–POF'98*, Berlin (Germany), pp. 33–38, 1998; A. M. Mescher, H. M. Reeve, and J. B. Dixon, "Transport phenomena in polymer optical fibers," in *Proc. Ninth International Conference on Plastic Optical Fibres and Applications–POF'00*, Boston MA, 26–31, 2000.
- [27] J. Arrue and J. Zubia, "Components choice to lengthen low speed plastic-fiber-optical communications links," in *Proc. Third International Conference on Plastic Optical Fibres and Applications–POF'94*, Yokohama (Japan), pp. 78–81, 1994.
- [28] M. Naritomi, "CYTOP[®] Amorphous Fluoropolymers for low loss POF," in *POF Asia-Pacific Forum-96*, Tokyo (Japan), 1996.
- [29] T. Kaino, "Absorption losses of low loss plastic optical fibers," *Jpn. J. Appl. Phys.*, vol. 24, 1661 (1985).
- [30] K. Koganezawa and T. Onishi, "Progress in perfluorinated GI-POF, LucinaTM," in *Proc. Ninth International Conference on Plastic Optical Fibres and Applications–POF'00*, Boston MA, pp. 19–21, 2000; Y. Takezawa, N. Taketani, S. Tanno, and S. Ohara, "Estimation method of intrinsic loss spectra in transparent amorphous polymers for POFs," *J. Appl. Pol. Sci.*, vol. 46, 1835 (1992).
- [31] T. Onishi, H. Murofushi, Y. Watanabe, Y. Takano, R. Yoshida, and M. Naritomi, "Recent progress of perfluorinated GI POF," in *Proc. Seventh International Conference on Plastic Optical Fibres and Applications–POF'98*, Berlin (Germany), pp. 39–42, 1998.
- [32] H. Murofushi, "Low loss perfluorinated POF," in *Proc. Fifth International Conference on Plastic Optical Fibres and Applications–POF'96*, Paris (France), pp. 17–23, 1996.
- [33] J. Gowar, *Optical Communications Systems*, 2nd ed., Prentice-Hall, London, 1993.
- [34] Y. Ohishi, S. Mitachi, T. Hanamori, and T. Manobe, "Optical absorption of 3d transition metals and rare earth element in zirconium fluoride glasses," *Phys. Chem.*, vol. 24, 77, 1983.
- [35] J. A. Jefferies and R. J. Klaiber, "Lightguide theory and its impurities in manufacturing," *The Western Electric Engineer*, vol. 26, pp. 13–23, 1980.
- [36] I. Pierrejean, J. Dugas, and G. Maurel, "Effects of structural anomalies of the PMMA core in the plastic optical fibers," in *Proc. First International Conference on Plastic Optical Fibres and Applications–POF'92*, Paris (France), pp. 96–100, 1992; H. Poisel, A. Hager, G. S. Ohm, V. Levin, and K. F. Klein, "P22 Lateral coupling to polymer optical fibers," in *Proc. Seventh International Conference on Plastic Optical Fibres and Applications–POF'98*, Berlin (Germany), pp. 114–116, 1998.
- [37] J. Meier, W. Liebert, W. Heinlein, W. Groh, P. Herbrechtsmeier, and J. Thies, "Time-domain measurements of step index plastic optical fibers," *Electron. Lett.*, vol. 23, 1208 (1987).
- [38] G. Jiang, R. F. Shi, and A. F. Garito, "Mode coupling and equilibrium mode distribution condition in plastic optical fibers," *IEEE Photon. Technol. Lett.*, vol. 9, no. 8, 1128 (1997).
- [39] E. L. Chinock, L. G. Cohen, R. D. Standly, and D. B. Keck, "The length dependence of pulse spreading in the CGW-Bell-10 optical fiber," *Proc. IEEE*, vol. 61, 1499 (1973).
- [40] T. Ishigure, E. Nihei, and Y. Koike, "Optimum refractive index profile for graded-index polymer optical fibers, toward gigabit data links," *Appl. Opt.*, vol. 35, no. 12, 2048 (1996).
- [41] R. Olshansky and D. B. Keck, "Pulse broadening in graded index optical fibres," *Appl. Opt.*, vol. 15, 483 (1976).
- [42] T. Ishigure, M. Satoh, O. Takanashi, E. Nihei T. Nyu, S. Yamazaki, and Y. Koike, "Formation of the refractive index profile in the graded index polymer optical fiber for gigabit data transmission," *J. Light. Technol.*, vol. 15, no. 11, 2095 (1997).
- [43] G. Yabre, "Theoretical investigation on the dispersion of graded index polymer optical fiber," *J. Light. Technol.*, vol. 18, no. 16, 869 (2000).
- [44] D. Gloge, "Optical power flow in multimode fibers," *Bell Syst. Technol. J.*, vol. 51, 1767 (1972).

- [45] T. Ishigure, M. Kano, and Y. Koike, "Which is a most serious factor to the bandwidth of GIPOF: Differential mode attenuation or mode coupling," *J. Light. Technol.*, vol. 18, no. 7, 959 (2000).
- [46] L. Blyler, "Material Science and Technology for POF," in *Proc. Eighth Conference on Plastic Optical Fibers and Applications-POF'99*, Chiva (Japan), pp. 196-200, 1999.
- [47] H. Guerrero, G. V. Guinea, and J. Zoido, "Mechanical properties of polycarbonate optical fibers," *Fiber and Integrated Optics*, vol. 17, 231 (1998).
- [48] J. Arrue, J. Zubia, G. Fuster, and D. Kalymnios, "Light power behavior when bending plastic optical fibers," *IEE Proceedings-Optoelectronics*, vol. 145, no. 6, 313 (1998).
- [49] J. Zubia, J. Arrue, and A. Mendioroz, "Theoretical analysis of the torsion induced optical effect in plastic optical fibers," *Opt. Fiber Technol.*, no. 3, 162 (1997).
- [50] Information Gatekeepers, Plastic optical fiber POF data book, pp. 47-49, 1993.
- [51] Lucina™ Technical Bulletin, Asaha Glass Company, 1998.
- [52] M. Sato, T. Ishigure, and Y. Koike, "Thermally stable high-bandwidth graded index polymer optical fiber," *J. Light. Technol.*, vol. 18, no. 7, 952 (2000).
- [53] H. Guerrero, J. Zoido, J. L. Escudero, and E. Bernabeu, "Characterization and sensor applications of polycarbonate optical fibers," in *Proc. Second International Conference on Plastic Optical Fibres and Applications-POF'93*, The Hague (Holland), pp. 166-170, 1993.
- [54] W. Daum, A. Hoffman, and U. Strecker, "Influence of chemicals on the durability of polymer optical fibers," in *Proc. Third International Conference on Plastic Optical Fibres and Applications-POF'94*, Yokohama (Japan), pp. 111-114, 1994.
- [55] A. Tagaya, Y. Koike, T. Kinoshita, E. Nihei, T. Yamamoto, and K. Sasaki, "Polymer optical fiber amplifier," *Appl. Phys. Lett.*, vol. 63, no. 7, 883 (1993).
- [56] A. Tagaya, S. Teramoto, E. Nihei, and Y. Koike, "High-power and high-gain organic dye-doped optical fibers amplifiers: Novel techniques for preparation and spectral investigation," *Appl. Opt.*, vol. 36, 572 (1997).
- [57] A. Tagaya, Y. Koike, E. Nihei, S. Teramoto, K. Fujii, T. Yamamoto, and K. Sasaki, "Basic performance of an organic dye-doped polymer optical fiber amplifier," *Appl. Opt.*, vol. 34, no. 6, 988 (1995).
- [58] G. D. Peng, P. L. Chu, Z. Xiong, T. W. Whitbread, and R. P. Chaplin, "Dye-doped step-index polymer optical fiber for broadband amplification," *J. Light. Technol.*, vol. 14, 2215 (1996).
- [59] K. Kuriki, T. Kobayashi, N. Imai, T. Tamura, and Y. Koike, "Organic dye-doped polymer optical fiber laser," in *Proc. Eighth International Conference on Plastic Optical Fibres and Applications-POF'99*, Chiba (Japan), pp. 171-174, 1999; K. Kuriki, T. Kobayashi, N. Imai, T. Tamura, S. Nishihara, Y. Nishizawa, A. Tagaya, and Y. Koike, "High-efficiency organic dye-doped polymer optical fiber laser," *Appl. Phys. Lett.*, vol. 77, no. 3, 331 (2000).
- [60] M. Laguesse and M. Bourdinaud, "Characterization of an X-ray detector with fluorescent plastic optical fiber readout," in *Proc. First International Conference on Plastic Optical Fibres and Applications-POF'92*, Paris (France), pp. 68-73, 1992; M. Laguesse and P. Rebourgeard, "Luminiscent optical fibers," in *Plastic Optical Fibres*, Club des Fibres Optiques Plastiques, Wiley, New York, 1997; Optectron, Polymer Optical Fibres Catalogue, 1996.
- [61] S. Teshima and H. Munekuni, "Multicore POF for High Speed Data Transmission," in *Proc. Seventh Conference on Plastic Optical Fibres and Applications-POF'98*, Berlin (Germany), pp. 135-142, 1998.
- [62] F. Mederer, R. Jäger, P. Schnitzer, H. Unold, M. Kicherer, K. J. Ebeling, M. Naritomi, and R. Yoshida, "Multi-Gb/s Grade-Index POF Data Link with Butt-coupled Single-Mode InGaAs VCSEL," *IEEE Photon. Technol. Lett.*, vol. 12, no. 2, 199 (2000).
- [63] M. Naritomi, "Model home project in Japan using GI-POF," in *Proc. Ninth International Conference on Plastic Optical Fibres and Applications-POF'00*, Boston MA, pp. 8-11, 2000.
- [64] R. Szweda, "Plastic optical fiber budgets the gap between glass and cooper," *Opto & Laser Europe*, vol. 72, 49 (2000).

- [65] Y. Koike, "Progress in GIPOF; Status of high speed plastic optical fiber and its future prospect," in *Proc. Ninth International Conference on Plastic Optical Fibres and Applications-POF'00*, Boston MA, pp. 1-5, 2000.
- [66] B. Chiron, "Highly efficient plastic optical fluorescent fibers and sensors," in *SPIE Proc. on Plastic Optical Fibres*, Boston MA, vol. 1592, pp. 86-95, 1991.
- [67] M. Laguesse and M. Bourdinaud, "Characterization of fluorescent plastic optical fibers for X-ray beam detection," in *SPIE Proc. on Plastic Optical Fibres*, Boston MA, vol. 1592, pp. 96-107, 1992.
- [68] Q. Zhou, "Development of chemical sensors using plastic optical fibers," in *SPIE Proc. on Plastic Optical Fibres*, Vol. 1592, pp. 108-113, Boston MA, 1991.
- [69] A. L. Bross, "Scintillating plastic optical fiber radiation detectors in high energy particle physics," in *SPIE Proc. on Plastic Optical Fibres*, Boston MA, vol. 1592, pp. 108-113, 1991.
- [70] S. Muto, H. Sato, and T. Hosaka, "Fluorescent-POF humidity sensor: theoretical and experimental analyses," in *Proc. Third International Conference on Plastic Optical Fibres and Applications-POF'94*, Yokohama (Japan), pp. 46-48, 1994.
- [71] K. Asada and H. Yuuki, "Fiber optic temperature sensor," in *Proc. Third International Conference on Plastic Optical Fibres and Applications-POF'94*, Yokohama (Japan), pp. 49-51, 1994.
- [72] E. Ito, J. Muramatu, and T. Kanazawa, "Plastic optical fiber thermosensor," in *Proc. Third International Conference on Plastic Optical Fibres and Applications-POF'94*, Yokohama (Japan), pp. 52-55, 1994.
- [73] J. Farenc, P. Pierre, and P. Destruel, "X-Ray sensor based on a fluorescent plastic optical fiber clad with a doped polymer," in *Proc. Third International Conference on Plastic Optical Fibres and Applications-POF'94*, Yokohama (Japan), pp. 56-59, 1994.
- [74] S. Hadjiloucas, L. S. Karatzas, D. A. Keating, and M. J. Usher, "Plastic optical fibers for measuring leaf water potential," in *Proc. Third International Conference on Plastic Optical Fibres and Applications-POF'94*, Yokohama (Japan), pp. 64-68, 1994.
- [75] K. H. Mertins and A. Meidinger, "Remote object sensor using plastic optical fibers and thick optical waveguides," in *Proc. Fourth International Conference on Plastic Optical Fibres and Applications-POF'95*, Boston MA, pp. 137-139, 1995.
- [76] S. Yamakawa, "Plastic optical fiber sensor array for computer visualization of organic gas concentration distribution," in *Proc. Fourth International Conference on Plastic Optical Fibres and Applications-POF'95*, Boston MA, pp. 140-145, 1995.
- [77] H.-A. Klok, H. Gankema, and M. Möller, "Polymer optical waveguides, ion-responsive fluorescent molecules and ion selective membranes-components for integrated optical chemosensors," in *Proc. Fourth International Conference on Plastic Optical Fibres and Applications-POF'95*, Boston MA, pp. 146-151, 1995.
- [78] K. Asada, H. Yuuki, and H. Hattori, "Application of POF to temperature sensors," in *Proc. Fourth International Conference on Plastic Optical Fibres and Applications-POF'95*, Boston MA, pp. 152-156, 1995.
- [79] N. Ioannides, D. Kalymnios, and I. Rogers, "A POF-based displacement sensor for use over long ranges," in *Proc. Fourth International Conference on Plastic Optical Fibres and Applications-POF'95*, Boston MA, pp. 157-161, 1995.
- [80] P. Destruel, J. Farenc, and P. Pierre, "Monitoring the electrode surface state of high voltage vacuum interrupters with X-ray sensitive plastic optical fibers," in *Proc. Fourth International Conference on Plastic Optical Fibres and Applications-POF'95*, Boston MA, pp. 162-166, 1995.
- [81] A. J. Schilk and T. W. Bowyer, "The use of scintillating plastic optical fibers for the detection of radioactive contamination," in *Proc. Fourth International Conference on Plastic Optical Fibres and Applications-POF'95*, Boston MA, pp. 171-176, 1995.
- [82] P. Gorodetzky, "Calorimetric measurements of elementary particle energy by means of plastic optical fibers," in *Proc. Fourth International Conference on Plastic Optical Fibres and Applications-POF'95*, Boston MA, pp. 177-180, 1995.
- [83] J. D. Weiss, "The pressure approach to fiber liquid level sensors," in *Proc. Fourth International Conference on Plastic Optical Fibres and Applications-POF'95*, Boston MA, pp. 167-170, 1995.

- [84] P. J. Scully, R. Chandy, R. Edwards, E. Lewis, D. F. Merchant, R. Morgan, N. F. Schmitt, and F. H. Zhang, "Plastic optical fiber sensors for environmental monitoring," in *Proc. Fifth International Conference on Plastic Optical Fibres and Applications-POF'96*, Paris (France), pp. 28–29, 1996.
- [85] K. F. Klein, S. Riesel, O. Schobert, and L. Veite, "Three color sensor for VIS and UV-A-region," in *Proc. Fifth International Conference on Plastic Optical Fibres and Applications-POF'96*, Paris (France), pp. 213–219, 1996.
- [86] J. J. Bayle and J. Mateo, "Plastic optical fiber sensor of refractive index, based on evanescent field," in *Proc. Fifth International Conference on Plastic Optical Fibres and Applications-POF'96*, Paris (France), pp. 220–227, 1996.
- [87] S. Hadjiloucas, D. A. Keating, and M. J. Usher, "Plastic optical fiber sensors for plant water relations," in *Proc. Fifth International Conference on Plastic Optical Fibres and Applications-POF'96*, Paris (France), pp. 228–237, 1996.
- [88] F. Baldini and S. Bracci, "Plastic optical fibers for the detection of pH in the foregut," in *Proc. Fifth International Conference on Plastic Optical Fibres and Applications-POF'96*, Paris (France), pp. 238–243, 1996.
- [89] N. Ioannides, D. Kalymnios, and I. W. Rogers, "An optimized plastic optical fiber (POF) displacement sensor," in *Proc. Fifth International Conference on Plastic Optical Fibres and Applications-POF'96*, Paris (France), pp. 251–255, 1996.
- [90] J. Niewisch, "POF sensors for high temperature superconducting fault current limiters," in *Proc. Sixth International Conference on Plastic Optical Fibres and Applications-POF'97*, Kauai HI, pp. 130–131, 1997.
- [91] S. Yamakawa, "Plastic optical fiber chemical sensor with pencil-shaped distal tip fluorescence probe," in *Proc. Sixth International Conference on Plastic Optical Fibres and Applications-POF'97*, Kauai HI, pp. 109–110, 1997.
- [92] K. Uchiyama, G. Vishnoi, M. Morisawa, and S. Muto, "Plastic optical fiber gasoline leakage sensor," in *Proc. Sixth International Conference on Plastic Optical Fibres and Applications-POF'97*, Kauai HI, pp. 140–141, 1997.
- [93] U. Steiger, "Sensor properties and applications of POF," in *Proc. Seventh International Conference on Plastic Optical Fibres and Applications-POF'98*, Berlin (Germany), pp. 171–177, 1998.
- [94] J. Zubia, J. Arrue, and J. Miskowicz, "Photoelastic effects of plastic optical fibers," in *Proc. Sixth International Conference on Plastic Optical Fibres and Applications-POF'97*, Kauai HI, pp. 134–135, 1997.
- [95] G. Garitaonandia, J. Zubia, U. Irusta, J. Arrue, and J. Miskowicz, "Passive device based on plastic optical fiber to determine the index of refraction of liquids," in *Proc. Seventh International Conference on Plastic Optical Fibres and Applications-POF'98*, Berlin (Germany), pp. 178–184, 1998.
- [96] M. Morisawa and S. Muto, "POF sensors for detecting oxygen in air and in water," in *Proc. Seventh International Conference on Plastic Optical Fibres and Applications-POF'98*, Berlin (Germany), pp. 243–244, 1998.
- [97] H. Kohzu, M. Morisawa, S. Muto, and C. X. Liang, "POF sensors for detecting leakage of fuel gases," in *Proc. Eighth International Conference on Plastic Optical Fibres and Applications-POF'99*, Chiba (Japan), pp. 234–237, 1999.
- [98] J. Zubia, O. Aresti, J. Arrue, J. Miskowicz, and M. López Amo, "Barrier sensor based on plastic optical fiber to determine the wind speed at a wind generator," in *Proc. Eighth International Conference on Plastic Optical Fibres and Applications-POF'99*, Chiba (Japan), pp. 260–266, 1999.
- [99] D. Pergesol, J. L. Lovato, and V. Minier, "Thermal diagnosis of medium voltage switchboards: a cost effective multi-point POF sensor," in *Proc. Eighth International Conference on Plastic Optical Fibres and Applications-POF'99*, Chiba (Japan), pp. 256–259, 1999.
- [100] M. Lomer, J. Etxebarria, J. Zubia, and J. M. López-Higuera, "In situ measurement of hydrofluoric and hydrochloric acid concentrations using POF," in *Proc. Ninth International Conference on Plastic Optical Fibres and Applications-POF'00*, Boston MA, pp. 164–167, 1999.